Snow depth time series retrieval by time-lapse photography: Finnish and Italian case studies

Bongio Marco[1], Ali Nadir Arslan[2], Cemal Melih Tanis[2], Carlo De Michele[1]

[1] Department of Civil and Environmental Engineering, Politecnico di Milano, Piazza Leonardo da Vinci 32, 20133, Milano, Italy

[2] Finnish Meteorological Institute, Erik Palménin aukio 1, P.O. Box 503, FI-00101 Helsinki, Finland

Correspondence to: Bongio Marco (marco.bongio@polimi.it)

Abstract. We tested the capability of the time-lapse photography to retrieve snow depth time series. Historically, the snow depth has been measured manually by rulers, with a temporal resolution of once per day, and a time-consuming activity. In the last decades, ultrasonic and/or optical sensors have been developed to obtain automatic and regular measurements with higher temporal resolution and accuracy. The Finnish Meteorological Institute Image Processing Toolbox (FMIPROT) has been used to retrieve the snow depth time series from camera images of a snow stake on the ground by implementing an algorithm based on the brightness difference and contour detection. We illustrated three case studies to highlight potentialities and pitfalls of the time-lapse photography to retrieve the snow depth time series: Sodankylä Peatland, a boreal forested site in Finland, Gressoney la Trinitè Dejola, and Careser dam, two alpine sites in Italy. In this study, we present new possibilities and advantages in the retrieval of snow depth in general, and snow depth time series in the specific, which can be summarized as follows: 1) retrieving the snow depth at high temporal resolution with an accuracy comparable to the most common method (manual measurements); 2) visual identification of errors or misclassifications; 3) estimating the spatial variability of snow depth; 4) correcting the under catch problem of pluviometer when this instrument is used. Root Mean Square Errors (RMSE) and Nash Sutcliffe Efficiency (NSE) are calculated for all three case studies comparing with estimates from both the FMIPROT and visual inspection of images directly. The NSE values were 0.917, 0.963, 0.916, while RMSE were 0.039 m, 0.052 m, 0.108 m respectively for Sodankylä, Gressoney and Careser. In terms of accuracy, the Sodankylä case study gave better results. The worst performances occurred at Careser dam located at 2600 m a.s.l. where extreme weather conditions and low temporal resolution of the camera occur, strongly affecting the clarity of the images.

1. INTRODUCTION

Seasonal snow has an important role in the Earth's climate system and a strong influence on its energy balance (Henderson et al. 2018), as well as it provides a fundamental contribution to the river discharge in catchments located in alpine and cold regions (Mastrotheodoros et al. 2020). Due to the inhomogeneous spatial distribution of snow, traditional in-situ measurement techniques can hardly provide exhaustive information about the snow variability (Lundberg et al. 2010). Remote sensing is becoming the most widespread technique to evaluate the snow cover (Takala et al. 2011; Da Ronco et al. 2020), the snow depth (De Michele et al. 2016; Avanzi et al. 2018; Lievens et al. 2019), and the snow water equivalent.

From the hydrological point of view, the main variable of snowpack is the snow water equivalent (SWE), rather than snow depth (SD), or snow density (ρ_s) (Avanzi et al. 2015). The snow water equivalent is a function of snow depth and snow density (De Walle and Rango, 2008) given in equation 1 below:

$$\mathrm{SWE}(t) = \mathrm{SD}(t)\frac{\rho_s(t)}{\rho_w} \quad (1)$$

where ρ_w is the density of water.

However, most of the historical information related to the snow are the manual measurements of snow depth. In fact, the depth is the simplest characteristic of snowpack, which can be easily detected with manual measurements within field campaigns (snow courses) (Pirazzini et al. 2018). This is particularly true in Alpine regions, and in correspondence of dam sites, where manual measurements by rulers, or snowboards (piece of plywood, painted white, that acts as a surface to collect snow, typically 16" x 16", or 16"x 24"). Manual measurements in the hydropower production are used to know the snowpack available in the melting season. Uncertainties related to snow depth measurements depend on the temporal and spatial resolution of the measurement methods. Manual measurements by rulers generally have daily resolution with $2-3$ cm accuracy. Ultrasonic sensors measurements have a finer temporal resolution (1 hour or less) with 1 mm accuracy. Satellite measurements are useful to estimate snow depth in a wide region with less accuracy (10 cm) and coarse temporal resolution (depending on orbit period).

The time-lapse photography has been used in literature to retrieve some characteristics of the snow such as: snow depth, snow canopy interception, snow settling, fractional snow cover on the ground, albedo, state of precipitation. Mainly applications were in remote areas, Greenland or Arctic Region, or in mountain regions, and related to the snow accumulation on glacierized areas (Christiansen 2001, Floyd and Weiler 2008, Farinotti et al. 2010; Parajka et al. 2012; Bernard et al. 2013; Garvelmann et al. 2013; Hedrick and Marshall 2014; Dong and Menzel 2017). In these studies, the principal aim is to show how the time-lapse photography could be used for investigating snow processes, but they were not specifically focused on the retrieval of snow depth.

Starting from 2001, continuous automatic digital photography was tested in high-Arctic Greenland to monitor snow-cover conditions from remote areas by Christiansen (2001). Daily photographs covered a 100 m transect through a seasonal snow patch, and thus on an annual basis also yields information on snow-cover duration in the different vegetation zones of the snow patch. Photographs, combined with measurements taken by Automatic Weather Stations, allowed to study snow wind induced redistribution on different thin snow-covered areas. Christiansen (2001) suggested that this method can be seen as a valid alternative to the traditional snow monitoring methods providing areal information and not only point measurements. Floyd and Weiler (2008) designed an automatic time-lapse photography network to monitor the state of precipitation (rain vs. snow), snow accumulation/ablation, canopy interception and unloading of snow from the canopy; they also defined an image analysis software which can calculate snow parameters from images.

Farinotti et al. (2010) tried to use the conventional oblique photography combined with a temperature index melt and accumulation model to infer the snow accumulation distribution of a small Alpine catchment. The inferred snow accumulation distribution was validated with in-situ measurements and correlations with topographic variables, such as curvature and slope, were founded. So here, the focus is on a better representation of SWE and its spatial variability within a distributed hydrological model in mountain complex terrain and time-lapse photography is only a tool to improve results.

Parajka et al. (2012) studied the potential of time-lapse photography to retrieve snow cover for hydrological purposes at small catchment scale. They designed and tested a monitoring system, which allowed multi-resolution observations of snow cover characteristics. They carried out investigations about snow cover, snow depth, and snowfall interception, both in the close area near the camera, and in a wider range. They tested the multi-resolution design at three sites in the eastern part of the Austrian Alps, using photographs at hourly time steps, showing that it is possible to process a large number of photos by using an automatic procedure for accurate snow depth readings. Using five stakes, it's possible to crosscheck snow depth estimations, omitting the largest and smallest readings, obtaining a robust estimate of the snow depth. The snow depth algorithm retrieval was not described in detail, but the routine calculated the visible markers from the top of the stake and then estimate the snow depth as a difference from the whole stake length. The accuracy was not so high because the snow stake had 10 cm markers and the camera had only 3 megapixels resolution. Any kind of sensor or manual measurements were used to compare the accuracy.

Bernard et al. (2013) installed, around the Austre Lovenbreen glacier basin (Norway, 79°N), automated digital cameras in the context of long-term monitoring snow and ice dynamics with high temporal and spatial resolution. Moreover, six camera stations were oriented to observe 96% of the glacierized area, monitoring in the hydrological year 2009 the snow cover evolution, studying the accumulation due to snowfall events and the ablation caused by precipitation, or warm temperature.

Garvelmann et al. (2013) defined a camera network to quantify snow processes such as: snow depth, snow canopy interception, albedo and the state of precipitation. About snow depth retrieval, they developed a semi-automatic approach, using images in which snow stakes with 10 cm red and black markers were visible. The main limitation was that they need to define the number of pixels of a 10 cm bar of the stake, and the whole stake length, with a procedure of cursor clicks which makes this procedure time-consuming. In addition, the accuracy was limited by the 10 cm snow stake markers, and the comparison was made only against visual observations. They reported an accuracy of 7.1 cm within the period December 2011 to April 2012.

Hedrick et al. (2014), within a test site, defined an automated, low-cost and safe snow depth retrieval system in avalanche terrain using time-lapse photography. For this purpose, they positioned two stakes painted with red color within the camera's view. They developed an algorithm that used pixel color intensities to automatically locate the snow surface for both the two stakes. The pixel counting algorithm clips each image to a small rectangle around the last known vertical pixel location of the marker base, then separates and smooths the blue channel of the RGB image for ultimate considerations. In fact, due to the high snow spectral albedo (that reflects most of the light in the near ultraviolet and blue visible spectrum), there was a large intensity gradient between depth marker and snow surface. This technique calculated a row wise RGB color minimum and the differences between two subsequent values. Snow surface was positioned near the maximum changing in the reflectivity level. Finally, the snow depth retrieval was obtained by subtracting the pixel row from the snow free image, then dividing by the number of pixels per centimeter for the particular marker. The snow depth value was compared with ultrasonic snow depth sensor and one LIDAR survey, showing a high underestimation of the implemented algorithm for the period between December 2012 and April 2013. Any accuracy parameter was reported, but only a visual comparison was described.

Dong et al. (2017) focused on the snow process monitoring in mountain forests with the time-lapse photography. They developed a semi-automatic procedure to retrieve the snow depth from the digital images, which exhibited high consistency with manual measurements and station-based recordings. To estimate the snow depth, they used images in which a stake with red and black markers, each 10 cm, was visible. The procedure required three different software: Photoshop to extract a measure line of three pixels width from each snow stake in each picture. Then these measure lines were imported in ArcGIS and converted in ASCII files. Finally, the brightness series were further processed in Excel to extract the snow depth information. In particular they calculated the maximum brightness of the top 80 cm of the snow stake and adding a fixed value (20) they defined the threshold to detect the snow surface. A pixel was assumed to represent the snow surface when the brightness values below this pixel was higher than the previous mentioned threshold. The regression model of the automatically

and manually interpreted snow depth values from the digital pictures were reported, which showed that the RMSE ranged from 0.011 to 0.019 m. Researchers should manually validate some abnormal values in accordance with the digital pictures obtained. In conclusions, some works about the snow depth retrieval from time-lapse photography are available, but presently, there is no a fully automatic procedure to retrieve the snow depth in real-time from the snow stake images, and thus time series.

In this study we present a fully automatic procedure to retrieve the snow depth in real-time, and snow depth time series, from time-lapse photography. The fully automatic procedure is based on an algorithm implemented within the FMIPROT, which uses the brightness difference between snowpack and stake's markers in digital images. We present the retrieval of snow depth time series for more than one hydrological year. We tested the procedure in three different sites, one in the Boreal forest in arctic region and two in Italian Alps. In the last two, existing configuration of camera and stake were not set out for retrieving of snow depth specifically. That's why we also investigated the proper geometric and parameter configurations of the camera-stake system, the sources of errors, and post-processing procedure corrections. We presented following results:

- how the accuracy of snow depth estimations can be increased using stakes with 1 cm spacing markers;
- proper geometric and parameter configurations of the camera-stake system;
- sources of errors and post processing procedure corrections;

The proposed fully automatic procedure can be taken as a reference for: (a) validating existing methods of snow depth retrieval, (b) comparing results in terms of amount and precipitation classification, (c) defining an alternative method to monitor dynamics of snowpack with high temporal resolution. The paper will be organized in the following sections: in section 2 method and algorithm are illustrated, in section 3 the case studies are described, in section 4 results are given, in section 5 a discussion of results is provided, in section 6 conclusions are drawn.

2. METHOD

In this section it is described how camera images (which show a snow stake with graduated markers) can be used to retrieve the snow depth. We introduce the FMIPROT, then we explain fully automatic procedure on the retrieval of snow depth, and finally we present a correction method to obtain a more affordable snow depth time series.

FMIPROT (Tanis et al. 2018) was developed for analyzing digital images from multiple camera networks for various applications such as vegetation phenology and monitoring of snow cover. This toolbox has a user-friendly graphical user interface (GUI) and can be used easily with only basic computing knowledge. Interface allows to easily download and/or read images from cameras network (online or offline) which provide continuous and widely series with the aim to monitor some environmental features such as phenology and snow.

Current features are automatic image downloading and handling, GUI based selection a region of interest (ROI), automatic analysis chain, GUI based plotting, creation of HTML reports with results on interactive plots, ROI based indices such as green fraction index (GF), red fraction index (RF), blue fraction index (BF), green-red vegetation index (GRVI), green excess index (GEI), snow cover fraction estimation with geo-rectification, snow depth estimation and time-lapse animation. FMIPROT is freely available at the website https://fmiprot.fmi.fi. In the next section, we will describe the fully automatic procedure for the snow depth retrieval developed from the protocol.

2.1 RETRIEVAL PROCEDURE OF SNOW DEPTH

The fully automatic procedure on the retrieval of snow depth is given in the Figure 1. The retrieval procedure of snow depth is articulated in eight steps: 1) **ROI IDENTIFICATION**: starting from an image without snow cover, with FMIPROT we selected the region of interest by drawing a polygon, which defined a quadrilateral around the snow stake. So, the pixel counting algorithm clips each image considering only pixels inside of this. In addition, we must define the real length of the whole ROI

in m. In most of the cases, it is better to define a polygon which includes the whole stake from the ground to the top level, but it is not mandatory, we have just to guarantee that the maximum snow depth value is less than the top of the ROI.

2) **GAUSSIAN FILTERING**: at each image it can be applied a Gaussian Filter based on the parameter σ, which smooths the brightness difference, reducing pixel noises. 3) **THRESHOLDING**: comparing the pixel value with a predefined brightness threshold T_S, we can classify each pixel as black or white (0 or 1). This threshold can vary widely, selecting different observation period, and we must define the best one able to reduce misclassifications. Related to this parameter is better to have a strong reflectance difference between the stake background and markers. We found that the best coloration of the stake is yellow or white for the background and dark color (i.e. black) for the markers. 4) **SEGMENTATION**: it is the process of partitioning a digital image into multiple segments. In our case this process defines the marker's contour with the edge detection. That's why is fundamental that stake must be graduated. In fact, the snow depth estimation resolution depends on the marker spacing. Markers with little distance can improve estimation accuracy, but we suggest remaining above 0.01 m because they must be identified clearly considering the distance between stake and camera. 5) **SHAPE FILTERING**: it consists on characterizing and filtering objects in binary scenes by its shape. Detected shapes that are not similar to square are filtered out, as they are not the markers but noise. 6) **MARKER HEIGHT**: the pixel row for each marker (d_i) is read from the remaining shapes. Note that the counting started from the upper part of the image. 0 means the top of the ROI. 7) **POSITION OF THE FIRST VISIBLE MARKER**: the snow depth layer is located near the first visible marker from the bottom of the stake, which is characterized by the minimum height value. Its pixel row is defined as:

$$S_D = min(H_i) \ \text{[n° of pixels]} \tag{2}$$

8) **RETRIEVING SNOW DEPTH**: the number of the pixels must be converted into the real depth multiplying it with the ratio between the real snow stake length (L_S) in meter and number of the pixel of the whole stake (H_S):

$$SD = S_D \frac{L_S}{H_S} \ \text{[m]}. \tag{3}$$

Counting pixel algorithm routine required the parameters definition, in particular for each case study we have to choose the best threshold (T_S) and the gaussian filter (σ), which allow to better estimate snow depth. The best parameters configuration is that allows to increase the brightness contrast between snowpack layer and stake's markers. Threshold can vary widely, because images have different resolutions, due to the different geometrical configuration and especially related to the different visibility conditions in terms of brightness and luminance. The same thing happened for the gaussian filter σ, which can assume values from 1 to 10. Firstly, we run the algorithm in a small period (10 days) searching for the best parameters configuration able to reproduce the snow depth visual estimated. After having found these values we run the algorithm for the whole observation period.

In Table 1, we reported the value of parameters used, for each case study. As we can see, depending on the maximum snow depth observed on the ground, we used different values of ROI length L_S: Careser dam is located near 2600 m a.s.l. so the expected maximum snow depth is near 2 m, thus L_S=2 m, at contrary at Sodankylä Peatland site, we observed a smaller value equal to 1 m, thus L_S=1 m. Related to the brightness threshold T_S we used values from 65 to 70, and for the gaussian filter σ values from 1 to 10.

We showed the best method consists of repeating the run of the algorithm with different parameters combination and defining an "ensemble" snow depth as the mean of those. This technique improves results, obtaining a more reliable snow depth time series.

Here the principal aim is not only the retrieval of the single snow depth value, but also the retrieval of snow depth time series with high accuracy. This issue is very important for hydrological purpose, but until now the application of time-lapse photography has been tested only for small time periods (months). We highlight that this procedure will be defined without

any snow depth measurements knowledge, in other terms, without data assimilation, because in most cases we have only images without real measurements.

The algorithm provides snow depth retrieval close to real values with high percentage, but sometimes it can fail, especially when atmospheric conditions were bad. In these cases, we found snow depth estimated values close to 0 or classified as Not-a-Number or affected by high biases. We defined a procedure to remove these incorrect values, running the algorithm five times with different parameters' combinations. In particular, we fixed the brightness threshold parameter T_S=70, and we defined five different values of the gaussian filter parameter σ from 1 to 5. Then each time series was used to define the "corrected snow depth time series". Now we reported all the steps necessary to run the retrieval algorithm: at first, we loaded the single snow depth time series estimated with fixed threshold Ts and gaussian filter parameter σ, called as: SD_O(t), where "O" means original. Then we removed errors and high biases, obtaining a more correct snow depth time series, which we will call as SD_C(t).

First of all, we suppose that in one hour was difficult to have a snowfall or melting much more than 0.02 m, so we reclassified as Not-a-Number $SD_O(t)$ if we have a difference more than 0.02 m to the previous or the following one. In some cases, we found a cluster of misclassifications, so values near Not-a-Number were suspicious, so we decided to reclassify each value near to a Not-a-Number as Not-a-Number itself. Summarizing we can write these conditions:

$$\text{if } (|SD_O(t) - SD_0(t-1)| > 2 \text{ cm OR } |SD_O(t+1) - SD_0(t)| > 2 \text{ cm}) \rightarrow SD_C(t) = \text{NaN} \quad (4)$$

$$if\ (SD_0(t) = \text{NaN}\ ) \rightarrow SD_c(t-1) = \text{NaN}\ \&\ SD_C(t+1) = \text{NaN} \quad (5)$$

In addition, in order to remove noise due to the optical sensor, we corrected the value at time t if this has an absolute difference more than 0.005 m (S) from the mean of the 12 (W) following and previous values. So we substituted the value at time t with a moving average of 24 values centered at time t. If we have NaN values inside this window, we did not consider them:

$$\text{if } \left(\left| SD_C(t) - \frac{1}{n}\sum_{t-\text{W}}^{t} SD_C(t) \right| > S\ \&\ \left| SD_C(t) - \frac{1}{n}\sum_{t}^{t+\text{W}} SD_C(t) \right| > S \right) \rightarrow SD_C(t) = \frac{1}{n}\sum_{t-\text{W}}^{t+\text{W}} SD_C(t) \quad (6)$$

where S is the maximum snow depth difference, equal to 0.005 m, and W is the window length of the moving average procedure, equal to 12 values. In this case n can be different from W, depending on how many NaN we found between t-W and t+W. In Figure 2, we reported results of these two previous steps, using images from Sodankylä Peatland with hourly resolution, from 1st January to 30th June 2017, and FMIPROT estimations obtained with parameters: $Ts = 70$ and $\sigma = 5$.

Finally we defined the final snow depth time series: the same correction (points 1 and 2) was repeated for each snow depth time series with five different values of parameter σ, from 1 to 5, which can be called as $SD_{C\,i}(t)$, where c means corrected and i goes from 1 to 5. The advantage of having 5 runs, was the possibility of compare the single value of one run $SD_{C\,i}(t)$ with the mean of the others 4, classifying as NaN the first if the difference was more than 0.001 m. In this way one single value was defined as reliable only if in the other 4 cases we observed more or less the same value. Summarizing we wrote the following condition:

$$\text{if } \left(\left| SD_{C\,i}(t) - \frac{1}{m}\sum_{j \neq i} SD_{C\,j}(t) \right| > 0.1 \text{ cm}) \right) \rightarrow SD_{C\,i}(t) = \text{NaN} \quad (7)$$

where m is equal to 4, i can take a value from 1 to 5, and j must be different from i. In this case m can assume values from 1 to 5 depending on how many values are different from NaN or 0.

Then, the "Mean Snow depth time series" was obtained as the mean value of the five $SD_{C\,i}(t)$ as:

$$SD_{MEAN}(t) = \frac{1}{n}\sum_{i=1}^{5} SD_{C\,i}(t) \quad (8)$$

The "Mean Snow depth time series" may still contain Not-a-Number values. In the case, there are not long time period with lack of data, we reclassified Not-a-Number values as the first previous valid value:

$$\text{if } SD_{MEAN}(t) = \text{NaN} \rightarrow SD_{MEAN}(t) = SD_{MEAN}(t - t_f) \quad (9)$$

where t_f is the number of time units before t where it is available a valid snow depth value. We underline that this condition works well only if images have fine temporal resolution and small period with lack of data. In Figure S4 we reported with colored dots the five corrected time series obtained with a fixed brightness threshold T_S and for different values of parameter σ from 1 to 5, after removing bias procedure previously defined (points 1 and 2), whereas with black dots and line the SD_{MEAN} time series as a result of the points 7 and 8. The period of analysis was the first half of 2017 and images are those collected from Sodankylä Peatland camera. Focusing on the SD_{MEAN} time series we showed that, despite that the original runs were characterized by lack of data or NaN values we defined a complete hourly time series. This procedure can give better results if we had images with high temporal resolution (less than one hour), because we can't observe high drop between two subsequent values also in case of high melting or snowfall rates, making the discarding phase much easier. Within the results section, this procedure will be evaluated in terms of accuracy and efficiency.

To better understand if this method is comparable in terms of accuracy and efficiency to the most common ones available in the literature, we calculated two indices: Root Mean Square Error (RMSE) and Nash Sutcliffe Efficiency (NSE). Those indices compared results obtained by FMIPROT, which will be indicated with the subscription "Sim", with the observed snow depth values indicated with the subscription "Obs". The last one was obtained by images inspection for all the three case studies. In the future, we plan to compare results also with in-situ measurements. We remind the definition of the two above mentioned accuracy parameters:

$$RMSE = \sqrt{\frac{1}{n}\sum_{i=1}^{n}(SD_{Sim}(i) - SD_{Obs}(i))^2} \quad (10)$$

$$NSE = 1 - \frac{\sum_{i=1}^{n}(SD_{Sim}(i) - SD_{Obs}(i))^2}{\sum_{i=1}^{n}(SD_{Obs}(i) - \overline{SD_{Obs}})^2} \quad (11)$$

where i means the temporal resolution, n is the total number of simulated values, SD_{Sim} is the simulated Snow Depth, and SD_{Obs} the Observed one (obtained by visual inspection of images). Moreover, SD_{Obs} is the mean observed value.

RMSE allows to calculate how much the single snow depth estimated value was different from the observed one, in average terms inside the whole observation period. It will be used to check the result's accuracy.

NSE compared the residual variance (numerator) with the observation variance (denominator). An efficiency value of 1 corresponds to a perfect match, but also values from 0 to 1 indicates that results are better predictors than the mean observed value. Generally, to indicate a sufficient quality has been suggested NSE values greater than a threshold from 0.5 to 0.65.

Unfortunately, this coefficient is sensitive to extreme values, so it is not optimal in case of observed values with high biases.

3. CASE STUDIES

SODANKYLÄ PEATLAND

As first case study, we considered the Sodankylä infrastructure, which monitors boreal/sub-arctic environmental and climate processes from below the surface to upper limits of the atmosphere and to space weather phenomena (Figure S1). In particular we referred to the images from the MONIMET Camera Network (Arslan et al. 2017; Peltoniemi et al. 2018, https://monimet.fmi.fi). In Sodankylä, there are a lot of cameras, but we selected the Peatland one because it was not affected by snow canopy interception, it is located in the prairie, it does not suffer from very strong windy conditions, so the relative

position between camera and stake remains the same. In addition, at the same site, there is also an automatic weather station as reported in Figure S1.

Images were collected at 30 minutes resolution from 8:00 AM to 6:00 PM, but generally in winter the first three images and those referred to the hours after 15:30 are totally dark, since the retrieval of snow depth strongly depends on their clarity. We decided to limit the use of images within a period of about 6 hours with a time resolution of 30 minutes. Images available are between 6/11/2015 and 28/04/2019.

The camera was located in front of a white snow stake with 1 cm spacing black markers. On the spacing it depends on the resolution of the snow depth retrieval because the algorithm cannot detect anything less than 1 cm. Each image has 2592 x1944 pixels with horizontal and vertical resolutions of 96 dpi. For images collected in the years 2015 and 2016, more stakes (two or three depending on the period) were deployed at different distances from the camera. The positioning of more than one stake enables to study the snow depth spatial distribution and also to compare the estimations between different stakes.

An ultrasonic snow depth sensor, available in the test site, collected data at 1-minute time resolution, used to validate and compare the results of the time-lapse photography. Generally, ultrasonic measurements suffer from a lot of noise due to the conversion of the travel time of the emitted and retrieved signals or the grass above the ground. A correction was automatically implemented and was based on air temperature data. To compare the results and reduce the noise, we defined a snow depth value every 30 minutes. This dataset is available at http://litdb.fmi.fi/suo0003_data.php, for the period 03/11/2011 to 27/03/2019. Having a fine temporal resolution, no lack of data for a long period, these snow depth measurements could be considered as a valid reference to test our method. Moreover, FMI personnel planned weekly field campaigns with the aim of retrieve snowpack conditions from 03/11/2011 to 28/04/2015. They measured snow water equivalent, snow density and snow depth.

We compared the ultrasonic snow depth measurements with the manual ones, over the overlapping period of observation: 2011-2015, in order to see how the ultrasonic measurements performs compared to the manual ones. In order to reduce noises of ultrasonic measurements, we aggregated these at hourly resolution. Figure 3 gives the comparison between manual measurements (red dots) and ultrasonic one (dark dots). Focusing on the years 2011 and 2014 we found agreement between the two methods of measurement, whereas in 2012 and 2013, we can see some differences. In 2012, ultrasonic snow depth sensor was characterized by some problems, prevented the measurements from being performed correctly. In 2015, ultrasonic snow depth sensor measured the highest snow depth peak which was smaller than the manual measurements. This situation was vice versa in 2013. In both 2013 and 2015, the accumulation season (typically winter), and the melting one (typically late spring) show a good agreement although there were differences in estimation peak values. In addition, we highlight that snow depth ultrasonic sensor were not affected by a persistent under/over estimation that can be a warning of instrument drift.

Caused by the poor resolution of the manual measurements and some periods with lack of data, we compared only 105 values. In addition, we cannot compare all the snow depth data series (ultrasonic, manual and FMIPROT estimations) because manual measurements were not available when the camera was installed. Finally, for each day in which we had both manual and ultrasonic snow depth sensor measurements, we calculated an RMSE equal to 0.045 m. By this, we retained reliable ultrasonic measurements and we used these measurements as reference for the years between 2015 and 2019 to compare the snow depth retrievals from time-lapse photography. Table 2 reports information about sensors, period of observation and time resolution used.

GRESSONEY LA TRINITE'

The second case study is located in Valle d'Aosta region (Italy), at an altitude of 1850 m (a.s.l.) where since 1927 the Meteorological Italian Society has measured the snow depth on the ground by rulers. This site can be considered a historical meteorological observatory of the snow depth retrieval in Italy due to the long data availability. In addition, from 2002 the

autonomous Valle D'Aosta region has installed an automatic weather station, with which they measured: precipitation (without heated pluviometer), temperature and relative humidity.

Figure S2 reports (from the right to left) Valle d'Aosta inside the Italian territory, Gressoney la Trinitè Dejola site, and a picture of the snow stake inside the meteorological observatory. Recently, from 01/09/2013 AINEVA (Interregional Association for snow and avalanche problems coordination) has positioned a snow stake with 10 cm spacing dark markers. The total length of the stake is 2 m and has a width of 10 cm. The camera is a Siap Micros model, with a height of 2 m above ground level and 10 m far from the stake. As shown in Figure S2, the snow stake was not positioned specifically for the remote sensing image processing purpose and it is affected by a not optimal geometrical configuration because there is a different distance between the camera and the top and the bottom of the stake. The importance of the positioning and optimal geometrical configuration will be described later in the section related to the discussion of results.

AINEVA, from 01/09/2013 saves images from the camera at hourly resolution from 6:00 AM to 6:00 PM. Especially in the winter season some images appear totally dark, so we decided to use only those taken from 8:00 AM to 15:00 PM. Dimension of the images are 1280x960 pixels, with horizontal and vertical resolutions of 96 dpi.

AINEVA operators made the visual estimation of the snow depth, saving in a spreadsheet file the snow depth value accumulated on the ground. From a personal communication with people who made these measurements, the camera is affected by a parallax effect, due to the relative distance between the height of the camera and the bottom of the stake. In addition, the real snow depth value cannot be retrieved simply reading the first marker not covered by snow because there is a heat transfer from the stake to the snowpack due to conduction and reflection of incident solar radiation. So, measurements reported by operators considered this effect, defining the real snow depth obtained as a cross between snow stake markers and a virtual line which links the snowpack accumulated on the ground at the left and right side of the stake (Figure 4 a).

In this way AINEVA operators defined two snow depth values for each day at 8:00 AM and 2:00 PM. We decided to use these values as a reference to compare the results obtained by our procedure. Figure 5**Errore. L'origine riferimento non è stata trovata.** gives for each day the two estimated values from 01/09/2013 to 26/04/2019.

From Fig.2, it is possible to see how for the years 2013-2014 and 2017-2018, the snow depth reached a value of 2.5 m overcoming the maximum length of the stake. In addition, many images are obstructed by snowflakes, which remained attached on the camera's view. So, in this case, AINEVA personnel used other information to define the snow depth time series above the ground. Because our aim is to compare and validate the snow depth values retrieved from digital images, we decided to discard years in which the reference value cannot be detected directly by visual inspection of images, focusing in the period between November 2014 and December 2017. As a period of validation, we selected the period between 2018-2019, as reported in the results section.

CARESER DAM

The third case study is located in Trentino region (Italy), the Careser dam, at an altitude of about 2600 m, near Careser glacier. The Civil Protection Agency installed a snow camera in 2014 with the aim of collecting snow data for hydrological purposes. In this region, there are a lot of sites in which manual measurements were taken every day. In fact, there are a lot of dams and ski areas, where private companies have an interest in monitoring of the snow availability during the winter season. In addition, AINEVA and Meteotrentino collected and spread daily information related to the snowpack such as snow depth and density to define the avalanche risk. Unfortunately, in Trentino region, as well as in the whole Italian territory, there are not many snow cameras, which can be used for our study. Figure S3 gives the location of the Careser dam and an image from the camera. Despite the fact that the camera was not specifically installed for a remote sensing image processing and retrieval of snow depth, we used this to test the potential of the time-lapse photography. The camera was located at 3 m above ground level, with a distance of about 6.5 m from the graduated stake that has a width of 15 cm, and colored in yellow with 1 cm spacing markers. The total length of the stake is 2 m. The camera model is Axis 214 PTZ, with a semispherical protection in Plexiglas.

Unfortunately, the temporal resolution is poor in this case, as they collected only 4 images per day at 5:00 AM, 8:00 AM, 11:00 AM and 2:00 PM. In most of the cases the first one at 5:00 am appears totally black, so we have discarded it.

The observation period goes from 01/01/2014 to 31/12/2018, but in some periods, there was a lack of data due to bad atmospheric conditions in which strong wind produced a camera rotation resulting images without snow stake. Other images which had to be discarded are those in which snowflakes remained on the camera's objective, making images totally grey or snow stake partially invisible. These problems occur when the camera was not protected properly. In fact, in most of the places where this technology was implemented, the camera was placed into a small wooden box. In addition, sometimes, the snow stake is positioned near a fence, that, especially in the melting season, enables a percolation toward the stake, which increases the snow melting. After the summer 2017, AINEVA replaced the camera with increased image resolution one. As a result of this change, the relative position between camera and stake was not the same for the whole observation period.

About images, from 2014 to the middle of 2017, they have 768x576 pixels with horizontal and vertical resolution of 96 dpi. Starting from November 2017, the number of pixels of each image was increased to 1920 x1080.

Unfortunately, in this case we have not any snow depth sensor, or snow field manual measurements, so to have a reference value to compare our estimations, we made visual estimations of the snow depth, simply opening each image, and watching the snow stake markers. In many cases the visual estimations were not so easy because an amount of snow remains attached on the snow stake. Another problem is the differential melting rate between snowpack close to the stake and at a distance of more than 1 m. This is caused by the high snow stake reflectivity related to the incoming sunlight, heat transmitted by conduction and the water percolation from the top to the bottom of the stake. This effect is hardly quantifiable and depending on the atmospheric conditions. So also, for the "visual estimation", this time series is affected by a noise which can be quantified in 5 cm. The "visual estimation" is obviously time consuming, because we have to open and read each image, but we are pretty sure that this kind of estimation is not affected by outliers or unreliable values. We have also to point out that the "visual estimation" is subjective and the same image can lead to different values by different observers. Figure 6 reports the snow depth daily time series obtained from visual estimation for the period between 1st November 2015 and 31st December 2018.

4. RESULTS

As a general comment, we can say that the algorithm of retrieval may fail in the snow depth detection when the geometrical configuration of the camera and the stake was not defined for this aim. For the two Italian case studies, the cameras were installed only for a rough evaluation of snow depth, and not planned for a quantitative monitoring of snowpack dynamic.

In Sodankylä Peatland case study, we used ultrasonic sensor, manual measurements and visual estimations from images as reference data for comparison. For the two Italian case studies, we must refer only on the visual estimations from images. In particular for Careser dam, we did not have any additional information, but for the Gressoney Dejola, the Meteorological Italian Society, visually estimated snow depth, with a "critical" snow depth definition, which means that they took in account the high melting that occurred close to the stake, and tried to remove the parallax effect, due to the different height between camera and the top of the stake.

SODANKYLÄ PEATLAND

In this case the algorithm works well because the stake was positioned closer to the camera, the images have more pixels showing the stake and appear clear, without high or low values of brightness and reflectivity. Moreover, it was positioned inside a small housing which can protect it against strongly windy conditions and possibility of obstruction of the camera's view caused by snowflakes. The stake much closer to the camera was enough to retrieve with enough temporal resolution and geometrical accuracy snow depth values. As mentioned in data description section, here we had images only after 2014, so to

check the reliability of the FMIPROT snow depth algorithm, we can only use the ultrasonic snow depth sensor, positioned close to the camera, because we did not have any other information, like manual measurements.

The comparison between retrieved and observed values of snow depth is reported in Figure 7, related to the period from 6/11/2015 to 27/03/2019. In particular we plotted retrieved values in blue dots, visual estimation of images with red dots, and Campbell ultrasonic measurements in black dots. The snow depth time series is correctly reproduced and good agreement between retrieved values and measurements has been found.

In general, visual estimations provide higher values, so we can observe an underestimation of the ultrasonic snow depth sensor and FMIPROT retrievals. Here it is interesting to highlight that the temporal resolution of FMIPROT retrievals is 30 minutes, within the daylight which starts from 9:00 AM and ends at 3:00 PM. Ultrasonic sensors measured snow depth at 10 minutes resolutions, and visual estimations were reported weekly. So, if the images were clear and without a long period with lack of data, we can build snow depth time series with high temporal resolution. About the accuracy, we calculated RMSE and NSE, comparing FMIPROT retrievals, with ultrasonic snow depth measurements and visual observation of images.

Comparing FMIPROT retrievals and ultrasonic snow depth sensor measurements, we obtained $RMSE_{FMI-U} = 0.096$ m, $NSE_{FMI-U} = 0.799$, while comparing FMIPROT retrievals with visual observation of images, we found $RMSE_{FMI-VO} = 0.085$ m, $NSE_{FMI-} = 0.881$. Visual observations are considered much more reliable because were obtained by a direct reading of the markers stake instead of the ultrasonic measurements, which is positioned much nearer to the camera and very far from the stake. We have also to highlight that the comparison with the ultrasonic snow depth sensor was done at hourly resolution, despite that those with visual inspections have weekly resolution. Another interesting issue is the number of misclassifications, or the inability of the FMIPROT algorithm to give a snow depth real value. In this case, NaN values were 2.91% of the images.

Building the snow depth time series in the first half of 2017

Thanks to the 30-min temporal resolution of the images and a period without lack of data, we tested the "smoothing" procedure defined in section 2 inside a 6-month period, on the first part of the year 2017, to obtain a complete snow depth time series without NaN values. Moreover, we repeated retrievals fixing the threshold parameter at 70 and varying the gaussian filter parameter σ from 1 to 5. The final snow depth time series was obtained by calculating the average of five retrievals. In Figure 8, we reported the comparison between the FMIPROT snow depth time series, visual estimation from images and the ultrasonic snow depth measurements.

As we can see from the Figure 8, we can build the snow depth time series with high temporal resolution and with high accuracy. As previously, considering as reference the visual snow depth estimations, we found for the ultrasonic snow depth sensor $RMSE_{US} = 0.052$ m, $NSE_{US} = 0.881$, while for the FMIPROT retrievals $RMSE_{FMI} = 0.039$ m, $NSE_{FMI} = 0.917$. With these values we can say that FMIPROT retrievals are much more accurate and efficient compared to the ultrasonic snow depth sensor values, and especially this happened in January and April.

These results are important because we can retrieve not only a single value of the snow depth with high accuracy, but we can build a snow depth time series, without lack of data. Moreover, these results were obtained without data assimilation procedure, which in most of the cases "force" the results knowing the real snow depth value. In addition, this procedure is completely automatic and low time consuming.

GRESSONEY LA TRINITE'

Inside the observation period which spans from 10/12/2013 to 20/05/2019 we selected the period from: 04/11/2014 to 31/12/2017 because in the other years the snow depth observations from AINEVA operators (Figure 4) report values higher than the stake length (2 m). In these cases, algorithm cannot retrieve correctly the snow depth, due to the fact that the snowpack overtakes the ROI, so we decided to discard them.

About the snow depth observed values, which will be used to compare our results, AINEVA operators for each day defined three values with a visual inspection of the images, respectively at 8:00 AM, 2:00 PM and 9:00 PM. The last one is equal to the last visible image for each day (AINEVA operator personal communication) so, as it is not known exactly at which time those measurements were referred, we avoided using those. For these reasons, having only 2 reference values for each day, to estimate the snow depth with FMIPROT we decided to select only two images per day, which corresponds at the same hours (8:00 AM and 2:00 PM). In most cases images appeared clear, without any lack of data, and defining the threshold values as mentioned in the algorithm section, we made the computations, using FMIPROT.

In addition, as mentioned in section 3, AINEVA operators defined a visual observation that considered the parallax effect, so, the algorithm detection of the first visible marker could be different from this visual estimation as shown in Figure 4a.

In this case, we had to define two different parameterizations to make retrievals due to the parallax effect, caused by the different distance which exists between the top and the bottom of the stake to the camera. Here the relative position between camera and stake was not optimal, because the camera was not positioned, in terms of height, at the middle of the stake. This situation leads to greater number of pixels corresponding to a marker for the top of the snow stake, compared to the bottom. As the consequence, considering a unique ROI, the parallax effect would cause a strong underestimation. In conclusion, when the snow depth is less than 0.3 m we used the following parametrization: $L_S = 0.3$ m , $T_S = 70$, $\sigma = 4$, when the snow depth is greater than 0.3 m we used: $L_S = 1.2$ m, $T_S = 70$, $\sigma = 4$.

Comparing the retrievals obtained by FMIPROT and values given by operators, we found that there was a strong difference between the two as reported in the scatterplot in Figure 9 . This showed a constant underestimation of the FMIPROT algorithm results. For this reason, in the following we will define a constant bias to correct our estimations. In addition, we calculated the ratio between observed and estimated values, as reported in Figure 10 in which we can see that the lowest values are those affected by the greater underestimations: this fact was expected because, due to the higher melting near the stake, if there was snowpack accumulated on the ground, the first visible marker could be near 0. In other terms when the real snow depth on the ground is near 0.1 m, the retrieval algorithm could fail. To better explain this fact, we reported also an image related to the data: 13/04/2016 (Figure 4b). Here the estimated snow depth reported by operator was: 0.24 m, but the algorithm gives 0.052 m because the stake was almost totally visible from the camera angle. As we will discuss in the following section, when the snow depth is less than 0.1 m, those images, and this geometric configuration didn't allow to estimate adequately snow depth. But we have to highlight that this is due to the imperfectly design of the relative position between camera and stake and not to the algorithm incapability.

So, these differences seem to be constant, and we decide to calculate the mean error, splitting the snow depth values between those greater than 0.3 m and others.

Considering observed values more than 0.3 m we found a mean error equal to 0.12 m, whereas for the values greater than 0.3 m, we found a mean error of 0.19 m.

Because our aim was to define a method to estimate snow depth which can be done automatically in the future without the long procedure of visual estimation from images, we defined a corrected snow depth retrieval time series in this way:

- If $SD_{Sim}(t) < 0.30$ m: $SD_{Sim\ Cor}(t) = SD_{Sim}(t) + 0.12$ m;
- If $SD_{Sim}(t) > 0.30$ m: $SD_{Sim\ Cor}(t) = SD_{Sim}(t) + 0.19$ m;

where $SD_{Sim}(t)$ is the original snow depth time series obtained by FMIPROT retrievals and $SD_{Sim\ Cor}(t)$ is the corrected values obtained by adding a correction factor (operator specific).

To verify visually the method's accuracy, in Figure 11, we reported the comparison between observed and retrieved values before and after correction. The new snow depth seems to be much closer to the observed one after this correction procedure.

We calculated also RMSE and NSE before the correction (BC) and after the correction (AC). In case of considering the original snow depth retrieval we obtained these accuracy parameters: $RMSE_{BC} = 0.171$ m, NSE_{BC} =0.609. After the correction procedure we increased the performances of retrievals obtaining these accuracy values: $RMSE_{AC} = 0.052$ m, NSE_{AC} =0.963.

In addition, we have to highlight also that in this case the number of the algorithm failings (i.e., when snow depth is equal to NaN) is only 1 among 1054. So, the percentage is less than 0.1%.

Moreover, to test the model reliability, we selected images between 10/11/2018 and 03/05/2019. Unfortunately, this period is not optimal to test our model because most of the time the snow depth on the ground was less than 0.1 m. Since we are interested to validate the method and check if the algorithm can retrieve with enough accuracy the snow depth, we referred only to the observed values greater than 0.1 m .

With this aim, we ran FMIPROT, and using the correction factor previously defined, we compared the results with the observed snow depth, obtaining the graph reported in Figure 12. We found $RMSE = 0.062$ m and $NSE = 0.771$. These results are comparable to those reported for the period 2015-2017.

This case study was interesting because, even though the geometrical configuration was not optimal, most of the images were discarded and the high melting close to the stake occurred, studying in a critical way the results and simply applying a constant correction factor, we can estimate snow depth values with good accuracy.

In this section, the correlation plot, helped us to define the method to correct the data, trying to minimize FMIPROT estimation errors. In the Sodankylä case study, we tried to correct measurements with another approach that is those reported in the Figure S4 in the supplement document, defining an ensemble of runs with different parameters. In this way we showed two different solutions to make our results more affordable.

CARESER DAM

In this case study, we have only three visible images per day at 8:00 AM, 11:00 AM and 2:00 PM. In addition, in the last year, camera was broken, so we could not use images to retrieve the snow depth. For these reasons we selected the period between 1/1/2016 to 11/06/2018.

As in Gressoney La Trinitè Dejola case study, also here we could not compare the FMIPROT algorithm estimations with manual or ultrasonic snow depth measurements. Thus, we referred to the visual estimation of images to validate our results. For the most of available images we estimated visually the snow depth by inspecting each image and recording in files the height of the first visible marker above the snowpack layer. We used these measurements as a reference to compare the results. We have already said that this method is not optimal, and it is affected itself by an error which can be quantified in 0.05 m . We remarked also the changing in the camera in summer 2017, this is the reason why we have to choose different parameters before and after that date. In fact, previous images have a worse pixel image resolution, but the camera's view is much more focused on the stake. After summer 2017, we can observe a better pixel's image resolution, but camera zoom decreased, and stake appeared much more far to the camera itself. In addition, we have to highlight the much more camera's stability occurred in the first period compared to the second one.

Initially we were worried about results because this site is located at an altitude near 2600 m, inside a prone windy area and with very bad climatic conditions in winter in terms of temperature and high snowfall. In addition, AINEVA and Meteotrentino collected images at 8:00 AM, 11:00 AM and 2:00 PM, and especially in spring the last one is not optimal because high sunlight levels.

In Figure 13 we reported the comparison within the observation period: 1/01/2016 – 31/12/2018.

These results were obtained defining as set of parameters: $L_S = 2$ m, $T_S = 67$, $\sigma = 10$, for the period until June 2017. After we changed the set of parameters: $L_S = 2$ m, $T_S = 68$, $\sigma = 3$.

We calculated the accuracy indexes between visual inspection and FMIPROT retrievals obtaining these results: $RMSE = 0.108$ m, $NSE = 0.916$.

Here we can see that algorithm was very successful, especially within the hydrological year 2016-2017 in which snow depth was not so high and there were few snowfall events and a subsequent rapid melting. Despite that this site was not defined with

the snow retrieval purpose, we obtained good results in terms of accuracy. The only problem here, was the camera use limitation due to the bad atmospheric conditions which characterized a mountain region. We have to highlight also that despite that the temporal resolution was poor, just 3 images per day, seems that we can follow the snowpack temporal variability with high accuracy. Probably, it would be better increasing the temporal resolution, which allows to have a snow depth time series with hourly resolution. The algorithm detected well the snow depth because markers of the stake were larger than other case studies, in fact here stake had a width of 0.2 m. So, applying a gaussian filter parameter greater than 1 we can avoid misclassification, and correctly detect stake's markers shape. We calculated the percentage of NaN over total images, which was equal to 1.5%.

5. DISCUSSION

Here we analyze firstly the causes of algorithm fail, and secondly configuration issues of the system camera-stake. As shown previously, especially when images had hourly resolution, in some cases the retrieval algorithm cannot provide correctly the snow depth value. Here we explain why that could happen and in the next section how we can solve these problems, improving the geometrical configuration. In the analysis of the three case studies we found eight sources of algorithm failing illustrated in Figure 14. Now we describe each of them: 1) Shadows projected on the snowpack, which falls inside the ROI. In some cases, especially when the sun was behind the camera, and some buildings or an automatic weather station or trees, were located near the camera, shadows on the snowpack surface was detected as a marker by the algorithm picking phase. This happened in all the three case studies. Panel 1 of Figure 14 shows this source of error, in which the sunlight highlighted the automatic weather station located near the camera projecting its shape above the snowpack. This induced the reading of the shadow's position as a first visible marker above the ground, strongly underestimated the snow depth, that, in this case, must be near 1 m. To avoid this problem, we suggest removing all the possible sources of shadows near stake and camera. 2) Footprint, which alters the snowpack in front of the stake and appears inside the ROI (Panel 2 of Figure 14). The same effect of that previously explained was caused by an alteration of the snowpack surface. Animals, men, or drops falling from the trees, can alter the surface, creating some discontinuities, which can be classified as a marker by the counting pixel algorithm phase. To avoid this problem, we suggest protecting the area close to the stake, making it inaccessible. 3) Obstruction of the camera's view (Panel 3 of Figure 14) Especially in case of extreme snowfall events, snowflakes can partially or totally cover both camera's view or some part of the stake obscuring the first clean marker which must be visible to correctly detect the snow depth. Here the only suggestion is to protect the camera against rainfall and snowfall events, positioning it inside a box which can be made with wood or steel with one side open or with a transparent window (Plexiglass or glass ones). 4) Pixel reflectance alteration: Due to excessive exposure of direct sunlight in the camera's objective, some images, lost its true colors becoming unreadable. This problem occurs rarely (Panel 4 of Figure 14), so it's difficult to find a geometrical design which can avoid this problem. 5) Rotation of the camera's view (Panel 5 of Figure 14): extreme windy conditions can cause the camera's rotation, and stake which disappears from the camera's view. To maintain the camera in the same position, it must be positioned inside a wooden or steel box as previously explained (point 3). 6) Blurred or opaque images (Panel 6 of Figure 14): in some cases, can happen that pixels cannot be distinguish among others, so from the algorithm point of view markers appear as the same as the background, making impossible its counting. 7) Wind snow drift (Panel 7 of Figure 14): strong wind velocity can carry snowflakes from the ground to the stake markers. In this case the markers became white and indistinguishable from the white background. 8) Direct sunlight in front of the camera and high reflectance above the snowpack (Panel 8 of Figure 14). In this case is not so clear why algorithm failed and what kind of protection has to be defined to avoid this problem.

Studying in detail results and causes of algorithm failing, we tried to define the proper geometrical configuration between camera and stake, highlighting the main characteristics which each single component must have:

- Relative position between camera and stake: the better configuration required that snow stake must be positioned as close as possible to the camera. In this case the algorithm can detect more easily markers position because more than one pixel can discretize one single marker. We suggest a maximum distance of 10 m. The camera's height has to be set in terms of reduce the parallax effect, so with a common stake of 2 m, it's enough a camera's height of 2 m. The rotation angle of the camera must guarantee the perpendicularity, avoiding the pixel size distortion. Between camera and stake it's better to remove all the possible obstructions such as branches of trees which can be identified as markers.
- Snow stake: we suggest a wooden stake, to reduce conductive heat transfer between stake and snowpack, limiting the sunlight reflectance on the snow. The background color must be yellow with black markers with 0.01 m spacing. Stake width must be 0.2 m and markers must cover half of that. It's better to make inaccessible the area near the stake, to avoid problems of snowpack alteration caused by human or animal footprint. To increase stake stability, it's better to fix it on a steel plate which in turn can be fixed on the ground (preferable on the rock) with at least 4 expandable anchors sleeves with quick settling cement. The ground or rocks surrounding the stake must be as flat as possible to avoid the gravitational movement of the first snowpack level, and the possibility of the horizontal translation of the stake.
- Camera: the image resolution is not so important if we respect an adequate distance from the stake, however we suggest using a camera with a high image resolution, say 5MP. It's mandatory to protect camera against wind, and precipitation events positioning it inside a wooden box of which one side must remain open or close with plastic or glass window.
- Connection with monitoring service: If characteristics of snowpack are required in real time there should be a permanent connection between the camera imaging storage and the monitoring service center. This can be power alimented thanks to a solar panel.
- Other instrumentations or field measurements: to cross correlate and validate algorithm estimations, periodically, it's mandatory compare algorithm estimations with manual measurements obtained by planned field campaigns. Additionally we suggest to place: (a) an automatic weather station with temperature sensor for removing some misclassification (as example highest melting rate if temperature was not more than 0°C), and (b) an ultrasonic snow depth sensor, which can be used when algorithm cannot detect in the correct way snow depth values. The last suggestion can be that of positioning more than one stake inside the camera's view and compared the algorithm estimations, defining different region of interest selecting one by one each stake.

Generally, working with images to detect if one pixel could be classified as snow, we defined a brightness threshold of 127. But in the three case studies it was found that a brightness threshold between 60 and 75 is better to detect the snowpack layer (probably because we were interested more in the marker's shape detection despite the single pixel classification). In addition, it was found that in most of the cases a gaussian filter sigma of 1 was good to retrieve correctly markers shape and position. Moreover, to define a reliable snow depth time series, it is better to repeat the analysis with different parameters configuration and take the mean value among them to remove all possible errors which can affect a single time series as explained for the Sodankylä Peatland case study.

In addition, as first image it is mandatory to have the whole snow stake not covered by snow, because we have to detect the right ROI (Region of Interest), which must have as the lower bound the ground level without snow. The highest contour level can be defined by the users remembering that it should be much more than the expected maximum snow depth in the accumulation season. Consequently, and coherently with the previous phase, at the ROI identification it has to be associated the real stake length in m.

6. CONCLUSIONS

The main aim of this study was to explore the capability of time-lapse photography method to retrieve snow depth time series in various snow conditions. Three case studies were considered: one in the boreal forest Finland, and two in the Italian Alps. The first case study was properly designed for retrieving the snow depth by camera images, while in the other two, cameras were set up for other purposes (a simple qualitative monitoring of the snow depth on the ground).

The results showed that, if the images were clear and the relative position between camera and stake allowed to detect stake's markers, the proposed algorithm implemented within FMIPROT was successful to estimate the snow depth. The agreement between estimations and visual inspection of the images was evaluated with the Nash Sutcliffe Efficiency, which reached values greater than 0.9, for all case studies. To evaluate the accuracy, the Root Mean Square Error was calculated, which was higher in the Careser dam site than in other two. This can due to: (1) the extreme weather conditions at 2600 m a.s.l. which may affect the camera's visibility and (2) the presence of the shadows above the snowpack layer, which can be classified as a stake's marker by the image's segmentation algorithm phase. There is a necessity to define the proper geometrical and parameter configuration for reducing the possible sources of estimation errors. Camera must be positioned at the same distance from the stake's ends and stake must be a wooden one of 15 cm width, with a yellow background color and black markers which covered half of that. Camera must be protected against extreme weather conditions (high wind velocity, intense rainfall or snowfall events) positioning it inside a wooden or steel box. All possible sources of shadows must be avoided. In Sodankylä case study, we compared the performances of the proposed algorithm with an ultrasonic snow depth sensor which measured the snow depth near the stake. In terms of NSE and RMSE, we found higher accuracy of the proposed algorithm against the ultrasonic Campbell sensor, assuming manual measurements as reference.

In conclusion, we underline some strength points of the proposed algorithm:

- High temporal resolution: depending on the camera's scan rate and storage data capability, we can build hourly or sub-hourly snow depth time series;
- High accuracy levels: if the geometrical configuration of camera-stake system and related infrastructures are perfectly designed, the proposed method estimates snow depth with accuracy levels comparable to the most commonly used (manual measurements, ultrasonic/optical sensors);
- Reliability: the percentages of algorithm failing are low and if some outliers are generated, we can easily detect and correct them with a post-processing procedure or simply opening the image and doing a "visual reading" of the first visible marker above the snow layer;
- Low cost: this can be considered as a low-cost solution with low maintenance costs;
- Remote sensing technique: can be easily extended in remote and dangerous areas such as mountain glaciers or polar regions in which currently there is a lack of data.

Our results indicate that the time-lapse photography has a good potential to retrieve snow depth time series. Future developments are necessary, such as improving the algorithm for reducing possible misclassifications and errors and may be possible upscaling solutions. The time-lapse photography can be a complementary solution to the satellite remote sensing for estimating snow depth automatically and remotely. It can be applied to many other applications such as estimating snowfall events, pluviometer under catch correction, snowfall and rainfall's splitting, estimating reservoir water levels or discharge or glaciers melting and monitoring in real-time lake or river's water levels in case of floods.

ACKNOWLEDGEMENTS

About the Finnish case study, we thank to FMI (Finnish Meteorological Institute) in particular at Anna Kontu and Leena Leppanen for the snow depth measurement data series. About the Gressoney Dejola, we thank Daniele Catberro of the SMI (Società Metereologica Italiana) for images and suggestions for data interpretations.

About the Careser dam case study, we thank Luca Froner who worked for Rete Sismica Trento and Civil Protection Agency of the Autonomous Province of Trento with webcam images.

AUTHOR CONTRIBUTIONS

Marco Bongio performed data analysis with advices from Ali Nadir Arslan and Carlo De Michele. The used retrieval algorithm on snow depth developed by Cemal Melih Tanis and implemented by Cemal Melih Tanis and Marco Bongio under supervising by Ali Nadir Arslan and Carlo De Michele. Marco Bongio wrote the manuscript with contributions from all co-authors.

Tables and Figures

Case study	Time period considered	ROI Length L_S [m]	Threshold T_S	Gaussian filter σ
Sodankylä Peatland	06/11/2015-28/04/2019	1.00	70	1
Gressoney La Trinitè	04/11/2014–31/12/2017 &10/11/2018-04/05/2019	1.20 or 0.3	70	4
Careser Dam	01/01/2016-26/05/2017	2.00	67	10
Careser Dam	04/11/2017-11/06/2018	2.00	68	3

Table 1. Snow depth algorithm parameters for each case study.

Case study	Sensor	Observation period	n° data	Resolution
Sodankylä Peatland	Ultrasonic (Campbell)	03/11/2011-27/03/2019	383963	10 minutes
	Manual measurement	03/11/2011-28/04/2015	105	Weekly
	Visual Estimation	07/11/2015-01/05/2019	129	Daily
	Camera	06/11/2015-28/04/2019	11604	30 Minutes
Gressoney La Trinitè	Visual Estimation (Aineva Operators)	04/11/2014-26/04/2019	1385	2-3 /Days
	Camera	04/11/2014-26/04/2019	1385	2-3 /Days
Careser Dam	Camera	01/01/2016- 01/06/2018	1714	3-4/Days
	Visual Estimation	01/01/2016- 01/06/2018	294	Daily

Table 2. Data description related to each case study with observation period and temporal resolution.

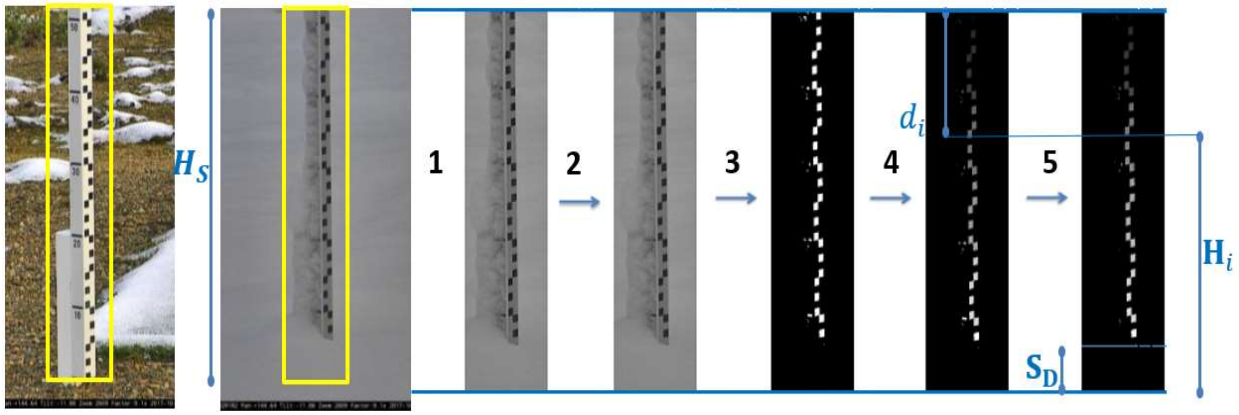

Figure 1. Snow depth retrieval procedure algorithm (SPICE Site - Sodankylä).

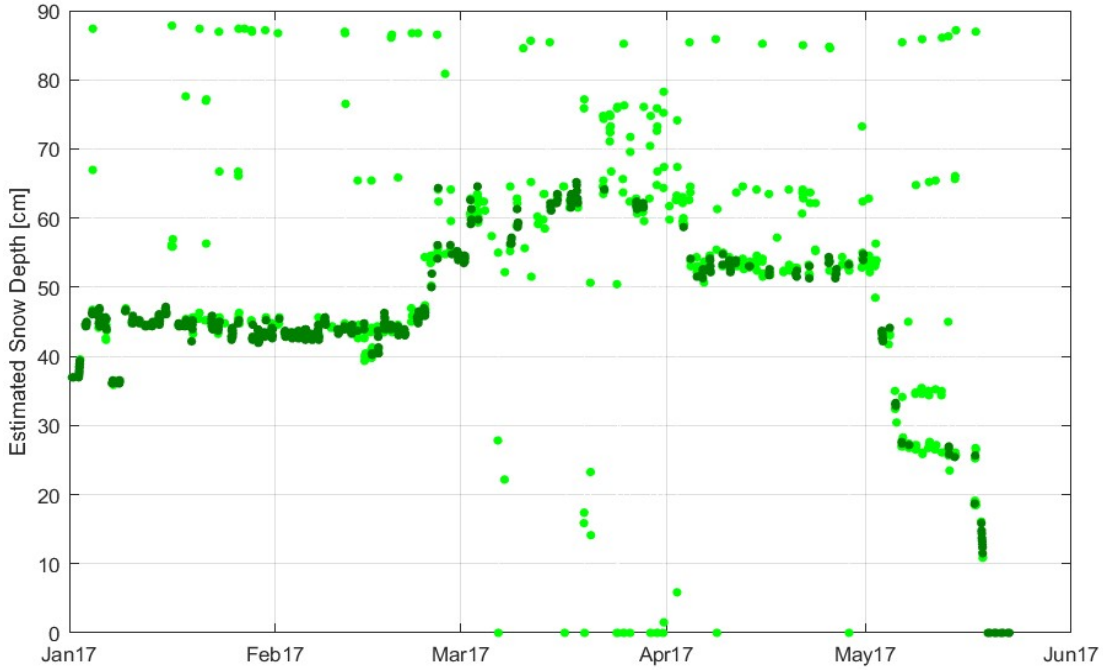

Figure 2. Sodankylä Peatland: Smoothing algorithm correction of FMIPROT applied to the snow depth estimate in the first half of 2017. In light green dots we reported the snow depth originally estimated by FMIPROT using $Ts = 70$ and $\sigma = 5$, with dark green dots the corrected snow depth time series.

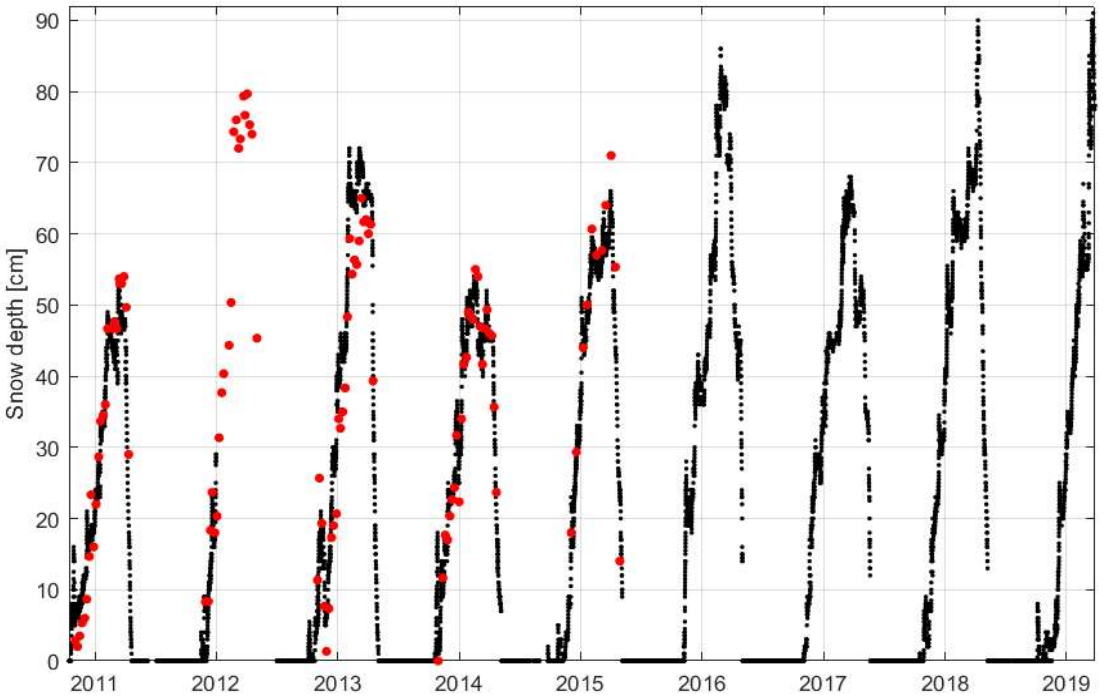

Figure 3. Sodankylä Peatland snow depth hourly time series collected by Campbell ultrasonic snow depth sensor (black dots) and manual measurements (red dots).

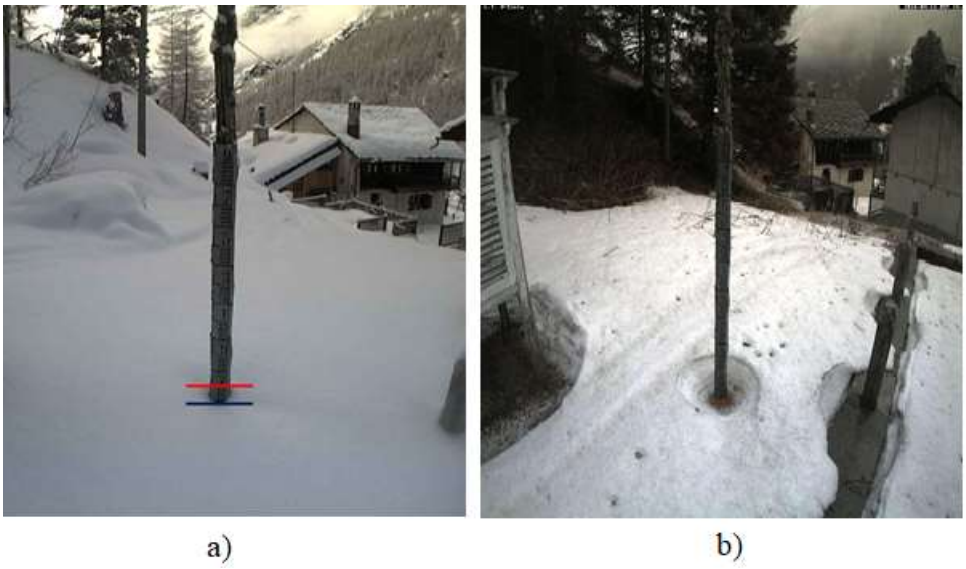

Figure 4. a) Images from Gressoney Dejola camera, taken at 8 AM of 09/02/2017. In red we marked the AINEVA Operator estimation, in blue the first selected marker from FMIPROT Algorithm. b) 13/04/2016 Image from Gressoney la Trinitè Dejola camera which shows the high melting rate close to the stake.

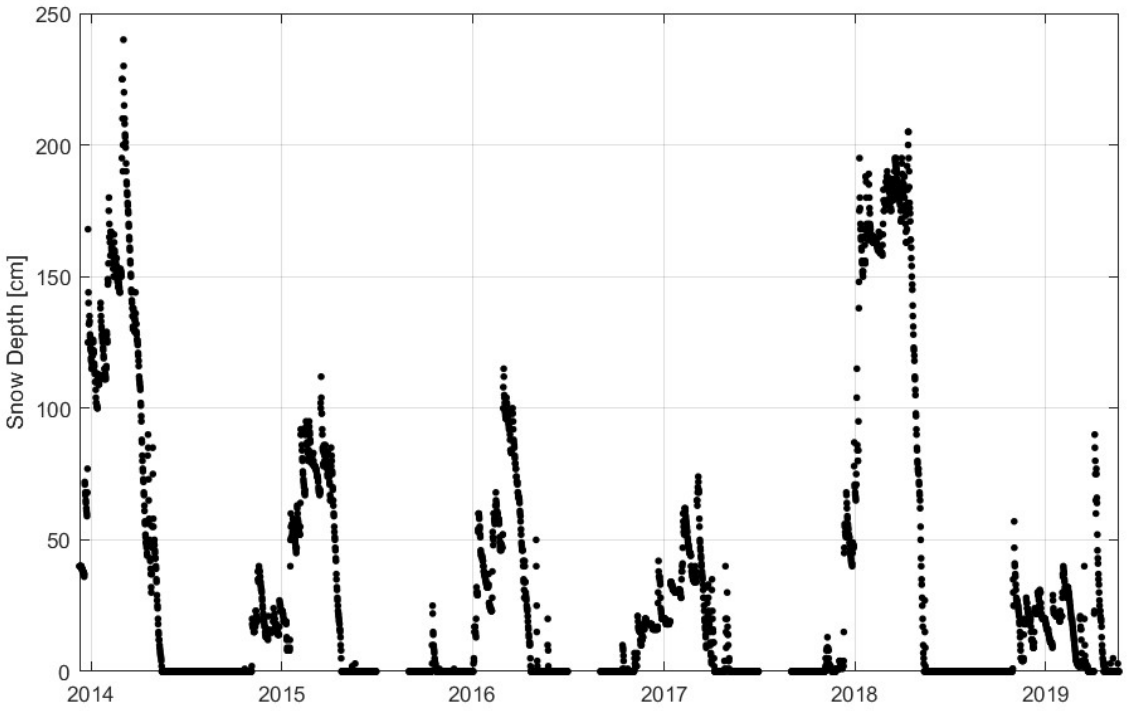

Figure 5. Gressoney La Trinitè Dejola: snow depth daily time series retrieval from camera images, at 8:00 AM and 2:00 PM, through visual estimation carried out by AINEVA operators, in the period 2013-2019.

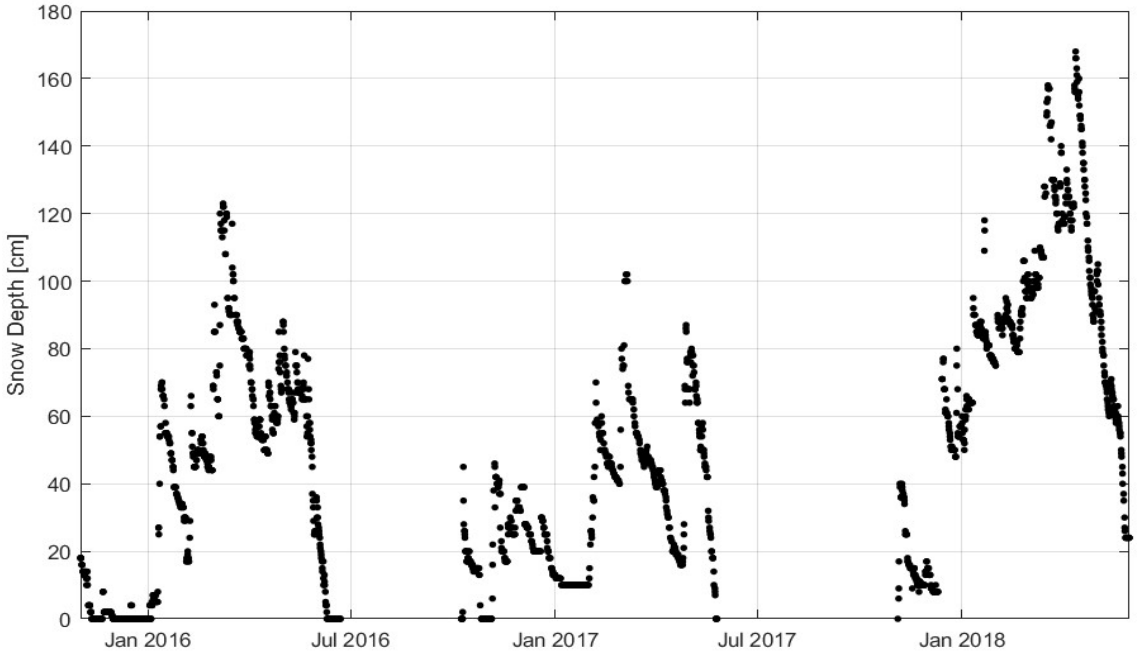

Figure 6. Careser dam: Snow depth daily time series from camera images through visual estimation in the period 2015-2018.

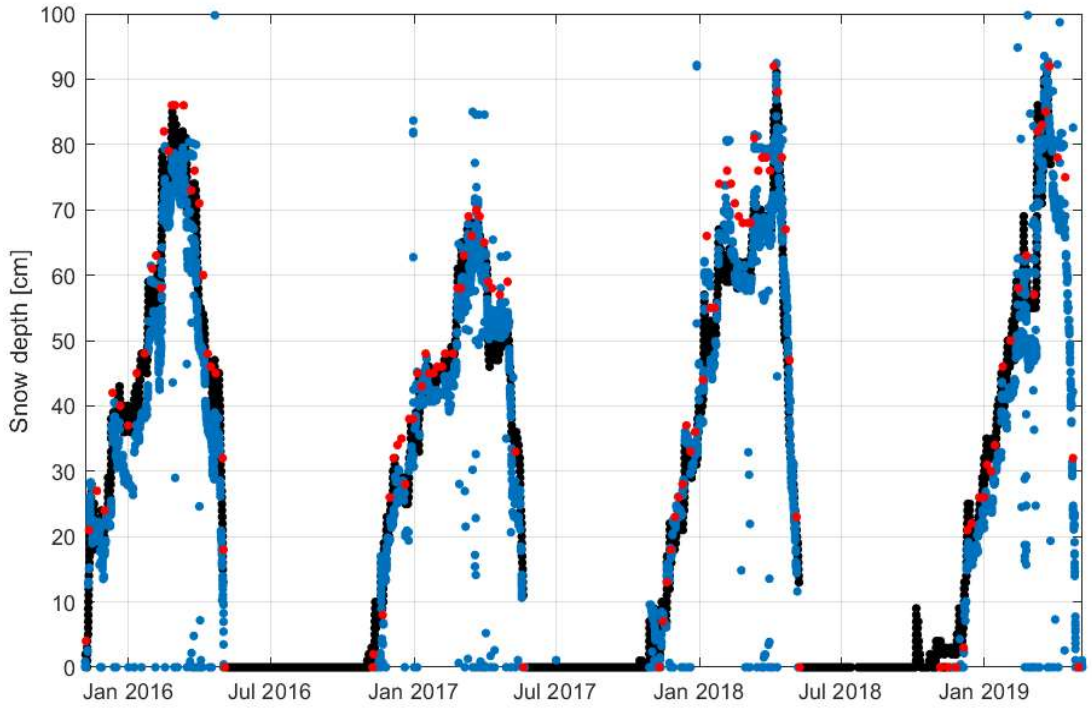

680

Figure 7. Sodankylä Peatland: Snow depth estimations comparison: Ultrasonic measurements (black dots), estimated by FMIPROT (blue dots), visual observations (red dots).

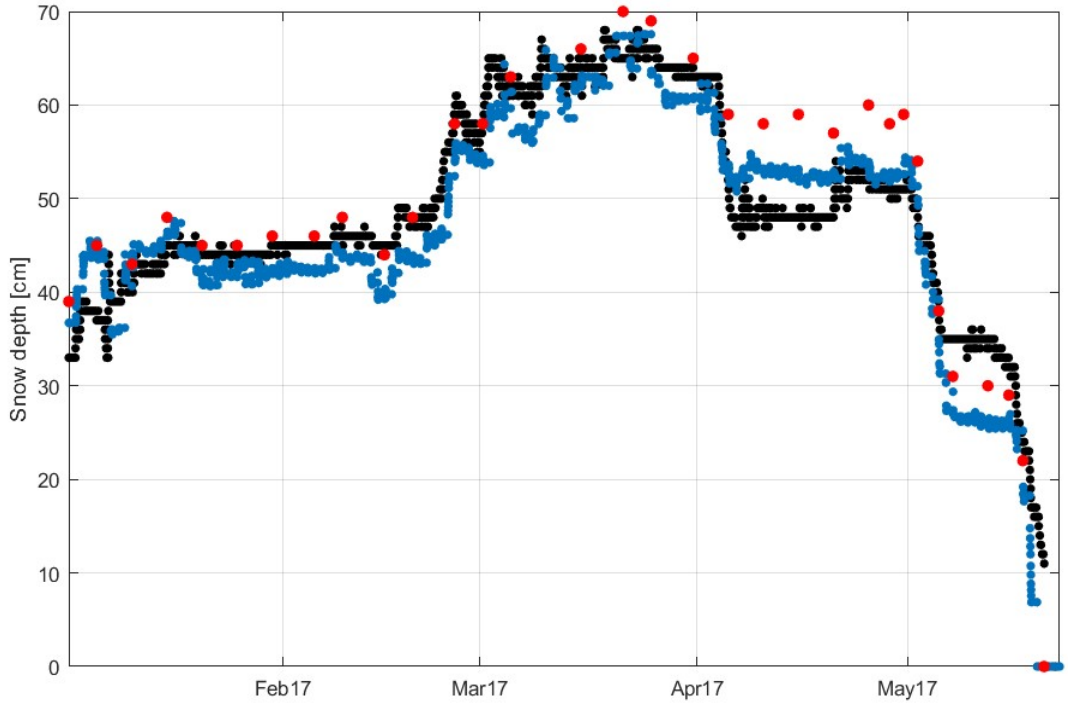

Figure 8. Sodankylä Peatland: Comparison between visual estimations (red dots), ultrasonic measurements (black dots), FMIPROT estimations (blue dots) in the first half of 2017.

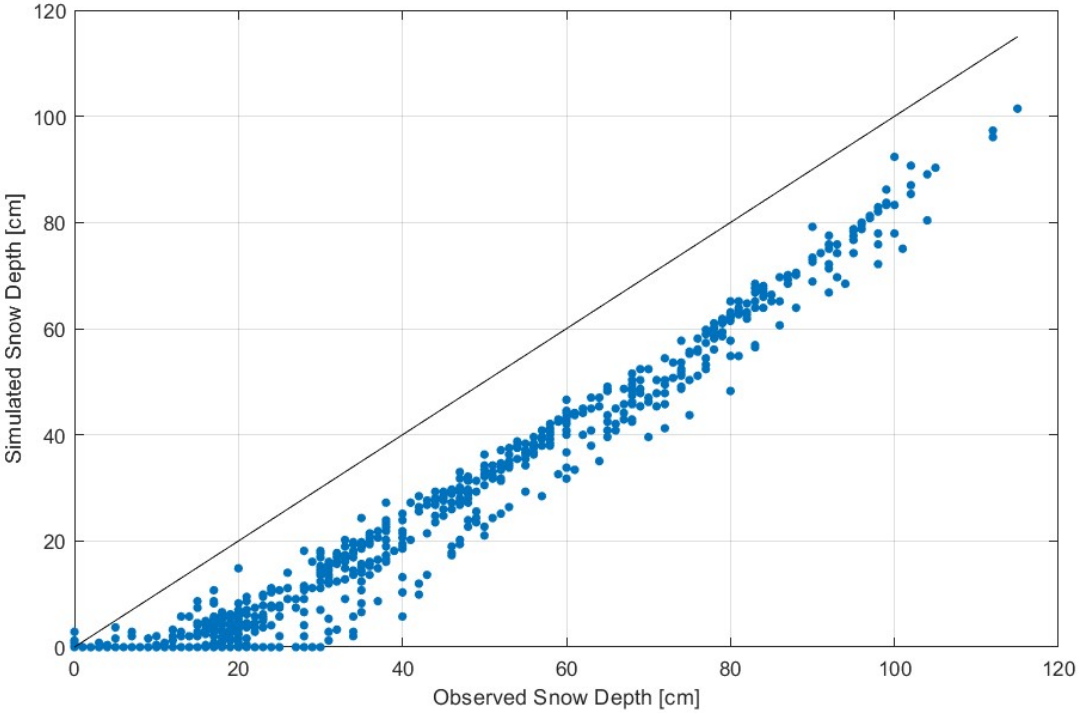

Figure 9. Gressoney La Trinitè Dejola: Scatterplot between estimated by FMIPROT (before correction procedure) and observed values.

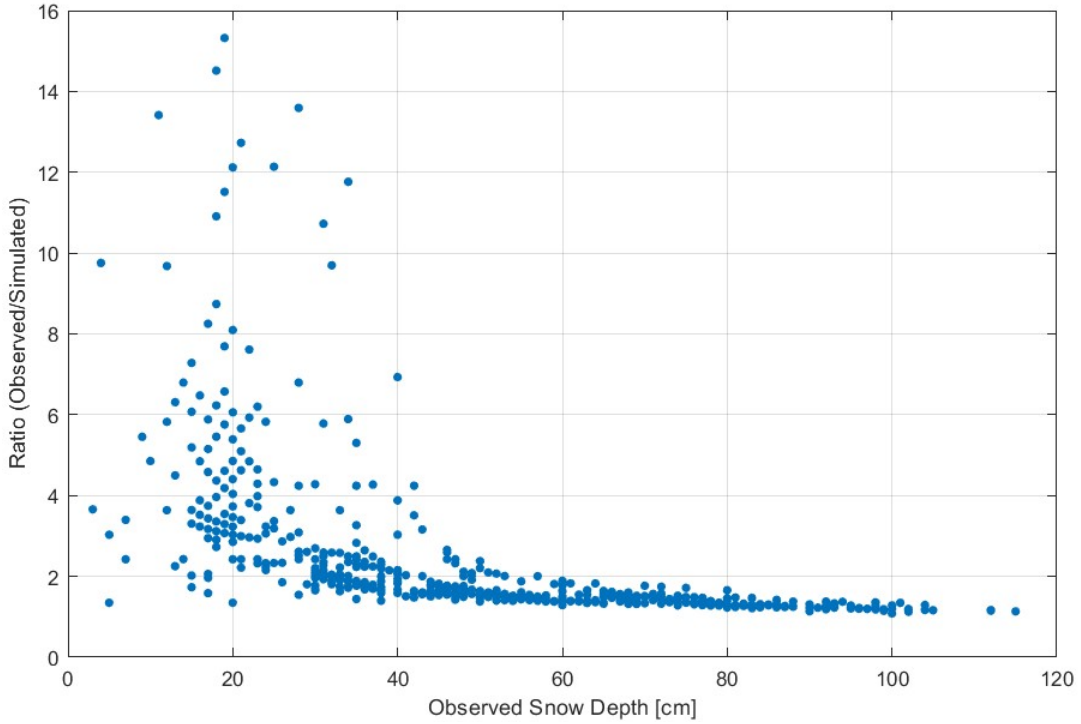

Figure 10. Gressoney La Trinitè Dejola: Ratio between observed and estimated snow depth values in the calibration period.

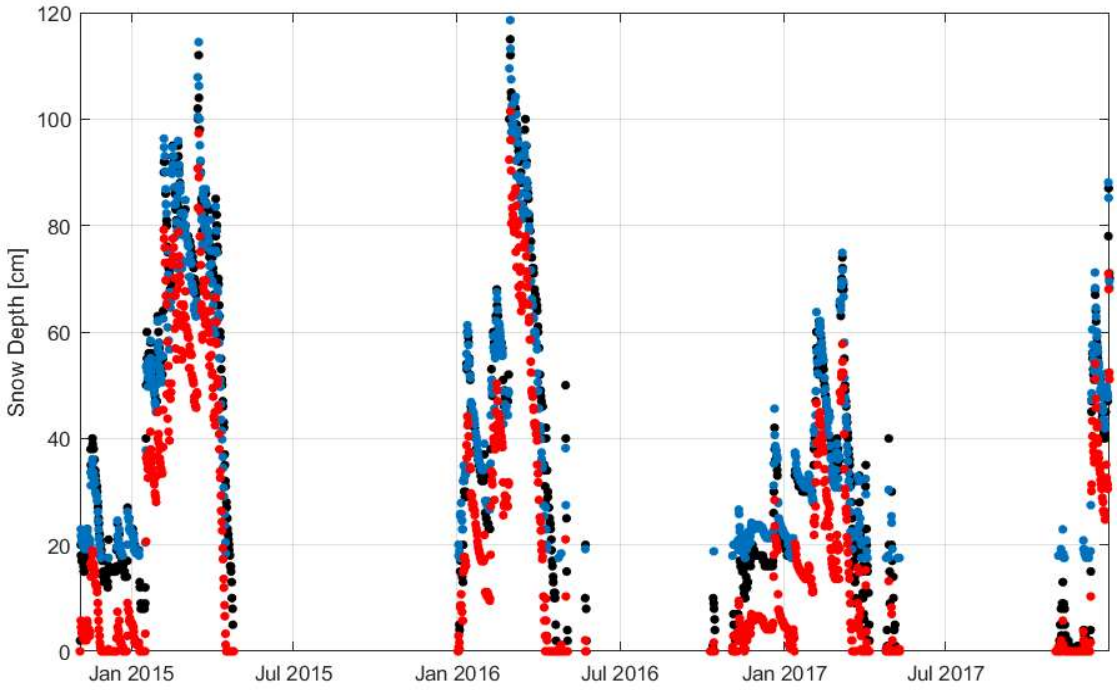

695

Figure 11. Gressoney La Trinitè Dejola case study: comparison between visual estimations (black dots) and estimated snow depth after (blue dots) and before (red dots) correction, in the calibration period.

700

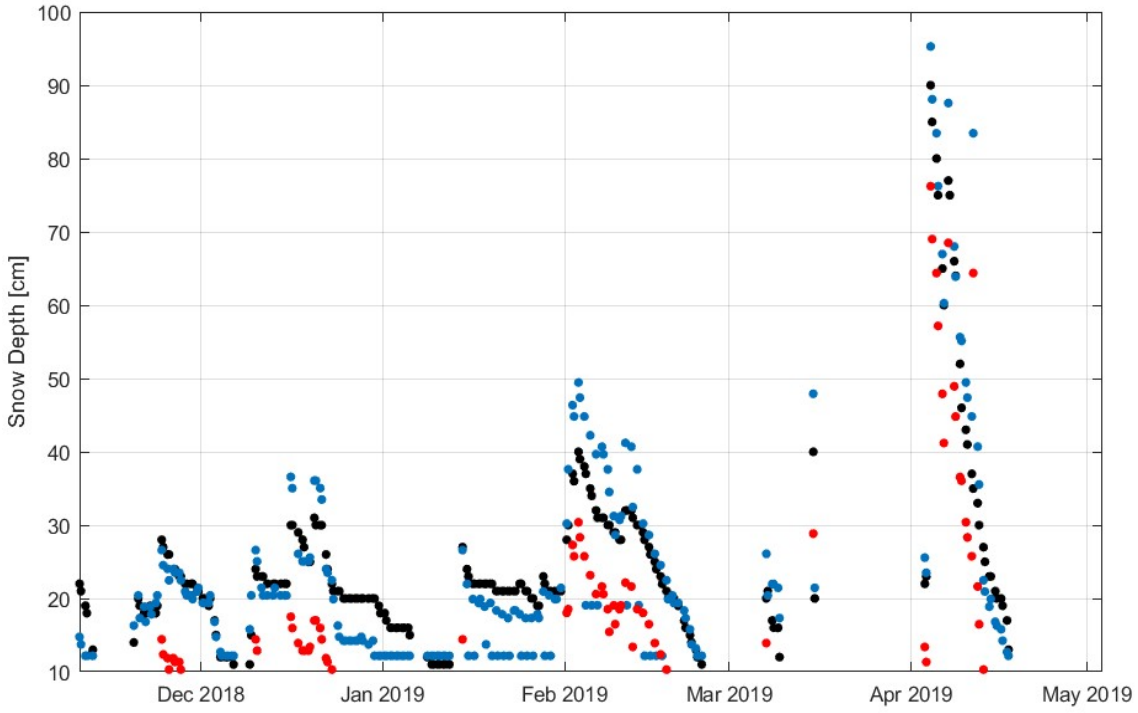

Figure 12. Gressoney La Trinitè Dejola: comparison between observed (black dots) and simulated snow depth after (blue dots) and before (red dots) correction, in the validation period (11/2018-05/2019).

705

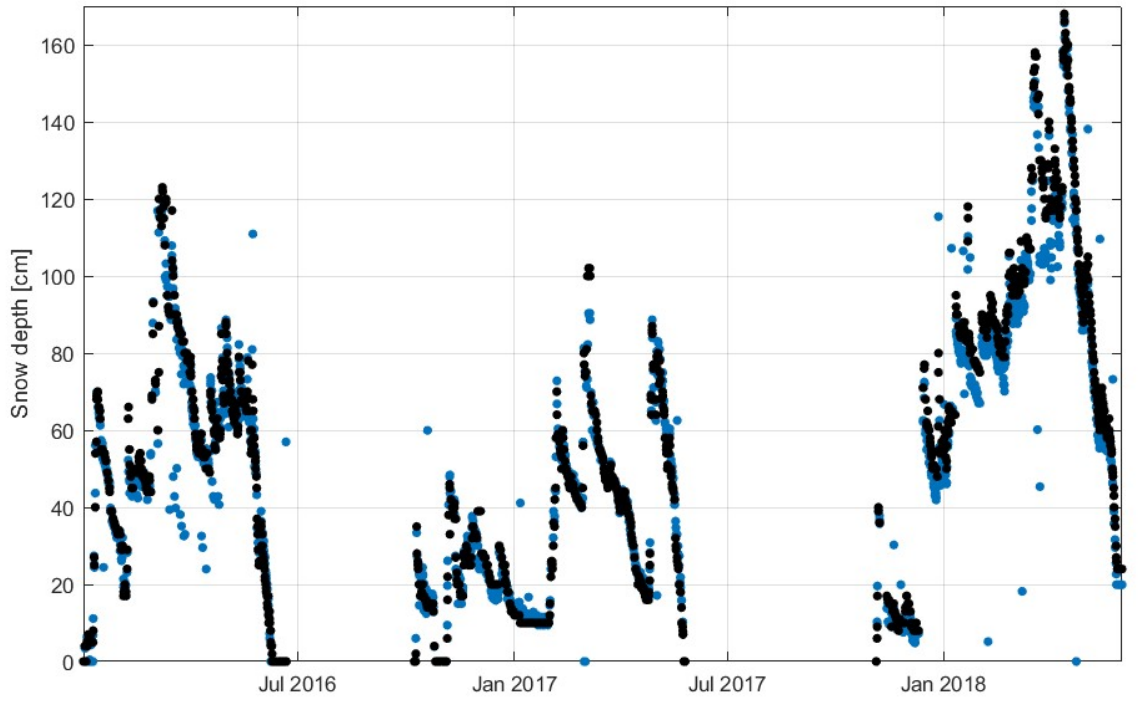

Figure 13. Careser dam case study. Comparison between snow depth retrieved by FMIPROT (blue dots) and visual estimation of images (black dots) for the period 1/1/2016-01/06/2018.

710

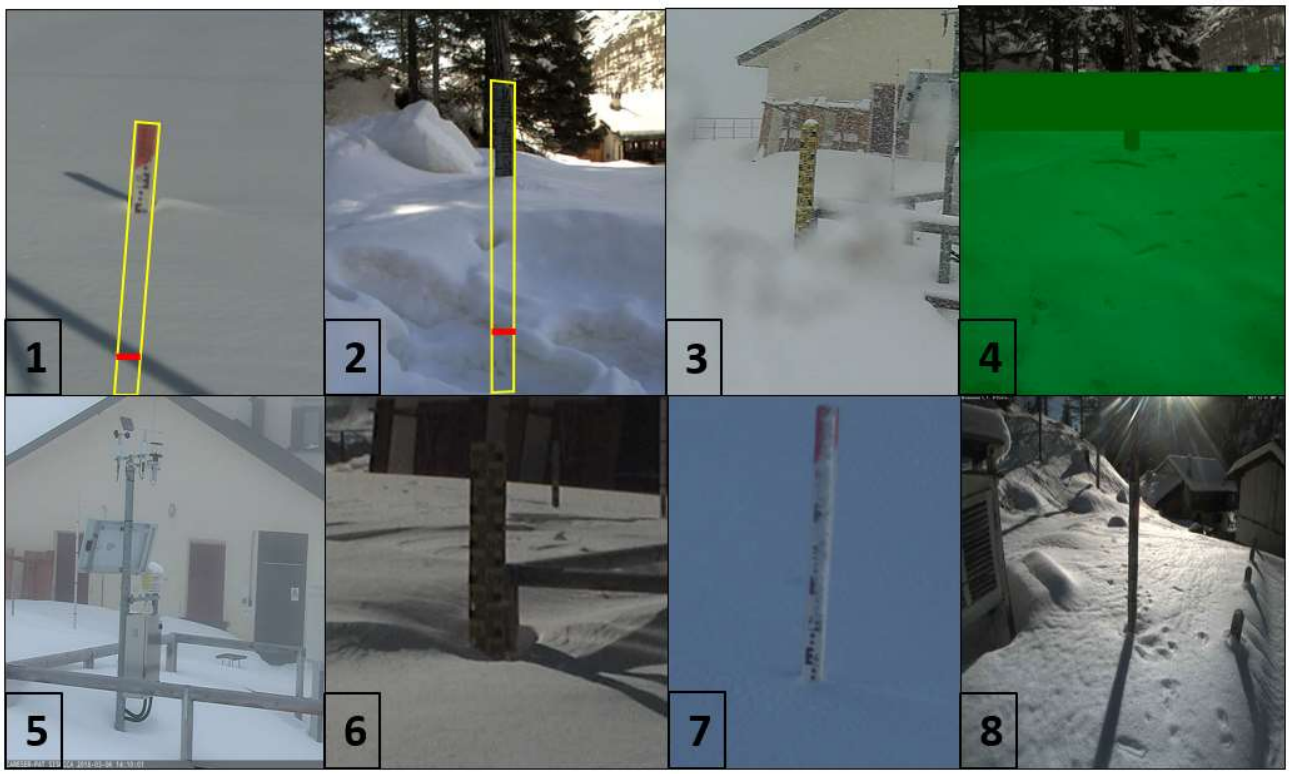

Figure 14. Sources of algorithm failing.

715

REFERENCES

Arslan, A., Tanis, C., Metsämäki, S., Aurela, M., Böttcher, K., Linkosalmi, M. and Peltoniemi, M.. Automated webcam monitoring of fractional snow cover in northern boreal conditions. Geosciences, 7(3), 55, https://doi.org/10.3390/geosciences7030055, 2017.

Avanzi, F., De Michele, C., Ghezzi, A., Jommi, C. and Pepe, M.. A processing–modeling routine to use SNOTEL hourly data in snowpack dynamic models. Advances in water resources, 73, 16-29, https://doi.org/10.1016/j.advwatres.2014.06.011 , 2014.

Avanzi, F., Yamaguchi, S., Hirashima, H. and De Michele, C.. Bulk volumetric liquid water content in a seasonal snowpack: modeling its dynamics in different climatic conditions. Advances in water resources, 86, 1-13, https://doi.org/10.1016/j.advwatres.2015.09.021, 2015

Avanzi, F., Bianchi, A., Cina, A., De Michele, C., Maschio, P., Pagliari, D., Passoni, D., Pinto, L., Piras, M. and Rossi, L.. Centimetric accuracy in snow depth using unmanned aerial system photogrammetry and a multistation. Remote Sensing, 10(5), 765, https://doi.org/10.3390/rs10050765, 2018.

Azar, A.E., Ghedira, H., Khanbilvardi, R. and Shahroudi, N. Combination of active and passive microwave to estimate snowpack properties using artificial neural networks in great lakes area, United States. Annual Conference Reno, Nevada, May 1-5, 2006, ASPRS 2006.

Bartelt, Perry, and Michael Lehning. A physical SNOWPACK model for the Swiss avalanche warning: Part I: numerical model. Cold Regions Science and Technology, 35(3), 123-145, https://doi.org/10.1016/S0165-232X(02)00074-5, 2002.

Bavera, D. and De Michele, C. Snow water equivalent estimation in the Mallero basin using snow gauge data and MODIS images and fieldwork validation. Hydrological Processes: An International Journal, 23(14), 1961-1972, https://doi.org/10.1002/hyp.7328, 2009.

Bavera, D., De Michele, C., Pepe, M. and Rampini, A. Melted snow volume control in the snowmelt runoff model using a snow water equivalent statistically based model. Hydrological Processes, 26(22),3405-3415, https://doi.org/10.1002/hyp.8376, 2012.

Bernard, É., Friedt, J.M., Tolle, F., Griselin, M., Martin, G., Laffly, D. and Marlin, C. Monitoring seasonal snow dynamics using ground based high resolution photography (Austre Lovénbreen, Svalbard, 79 N). ISPRS Journal of Photogrammetry and Remote Sensing, 75, 92-100, https://doi.org/10.1016/j.isprsjprs.2012.11.001 ,2013.

Brun, E., David, P., Sudul, M. and Brunot, G. A numerical model to simulate snow-cover stratigraphy for operational avalanche forecasting. Journal of Glaciology, 38(128), 13-22, https://doi.org/10.3189/S0022143000009552, 1992.

Bühler, Y., Adams, M. S., Bösch, R., and Stoffel, A.: Mapping snow depth in alpine terrain with unmanned aerial systems (UASs): potential and limitations, The Cryosphere, 10, 1075-1088, https://doi.org/10.5194/tc-10-1075-2016, 2016.

Carmagnola, C. M., Morin, S., Lafaysse, M., Domine, F., Lesaffre, B., Lejeune, Y., Picard, G., and Arnaud, L.: Implementation and evaluation of prognostic representations of the optical diameter of snow in the SURFEX/ISBA-Crocus detailed snowpack model, The Cryosphere, 8, 417-437, https://doi.org/10.5194/tc-8-417-2014, 2014.

Che, T., Li, X., Jin, R., Armstrong, R., & Zhang, T.. Snow depth derived from passive microwave remote-sensing data in China. Annals of Glaciology, 49, 145-154. doi:10.3189/172756408787814690, 2008.

Christiansen, H. Snow-cover depth, distribution and duration data from northeast Greenland obtained by continuous automatic digital photography. Annals of Glaciology, 32, 102-108. doi:10.3189/172756401781819355, 2001.

Da Ronco, P., Avanzi, F., De Michele, C., Notarnicola, C., & Schaefli, B., Comparing MODIS snow products Collection 5 with Collection 6 over Italian Central Apennines, International Journal of Remote Sensing, 41:11, 4174-4205, doi: 10.1080/01431161.2020.1714778, 2020.

De Michele, C., Avanzi, F., Ghezzi, A., and Jommi, C.: Investigating the dynamics of bulk snow density in dry and wet conditions using a one-dimensional model, The Cryosphere, 7, 433-444, https://doi.org/10.5194/tc-7-433-2013, 2013.

De Michele, C., Avanzi, F., Passoni, D., Barzaghi, R., Pinto, L., Dosso, P., Ghezzi, A., Gianatti, R., and Della Vedova, G.: Using a fixed-wing UAS to map snow depth distribution: an evaluation at peak accumulation, The Cryosphere, 10, 511-522, https://doi.org/10.5194/tc-10-511-2016, 2016.

DeWalle, D.R. and Rango, A. Principles of snow hydrology, Cambridge University Press, Cambridge, United Kingdom, 2008.

Dong, C. and Menzel, L. Snow process monitoring in montane forests with time-lapse photography. Hydrological Processes, 31(16), 2872-2886, https://doi.org/10.1002/hyp.11229, 2017.

Farinotti D., Magnusson, J., Huss, M. and Bauder, A. Snow accumulation distribution inferred from time-lapse photography and simple modelling. Hydrological processes, 24(15), 2087-2097, https://doi.org/10.1002/hyp.7629, 2010.

Floyd W., and Weiler, M. Measuring snow accumulation and ablation dynamics during rain-on-snow events: innovative measurement techniques. Hydrol. Process., 22: 4805-4812. https://doi.org/10.1002/hyp.7142, 2008.

Garvelmann, J., Pohl, S., and Weiler, M.: From observation to the quantification of snow processes with a time-lapse camera network, Hydrol. Earth Syst. Sci., 17, 1415-1429, https://doi.org/10.5194/hess-17-1415-2013, 2013.

Goodison, B.E., Louie, P.Y. and Yang, D. WMO solid precipitation measurement intercomparison (p. 212). Geneva, Switzerland: World Meteorological Organization, 1998.

Hedrick, A.R. and Marshall, H.P. Automated Snow Depth Measurements in Avalanche Terrain Using Time-Lapse Photography. Proceedings of International Snow Science Workshop 2014 Proceedings, Banff, Canada, 2014.

Helfricht, K., Hartl, L., Koch, R., Marty, C., and Olefs, M.: Obtaining sub-daily new snow density from automated measurements in high mountain regions, Hydrol. Earth Syst. Sci., 22, 2655–2668, https://doi.org/10.5194/hess-22-2655-2018, 2018.

Henderson, G. R., Peings, Y., Furtado, J. C. & Kushner, P. J. Snow-atmosphere coupling in the Northern Hemisphere. Nat. Clim. Change 8, 954–963, 2018.

Kochendorfer, J., Rasmussen, R., Wolff, M., Baker, B., Hall, M. E., Meyers, T., Landolt, S., Jachcik, A., Isaksen, K., Brækkan, R., and Leeper, R.: The quantification and correction of wind-induced precipitation measurement errors, Hydrol. Earth Syst. Sci., 21, 1973-1989, https://doi.org/10.5194/hess-21-1973-2017, 2017.

Legates, D.R. and Willmott, C.J. Mean seasonal and spatial variability in gauge-corrected, global precipitation. International Journal of Climatology, 10(2), 111-127, https://doi.org/10.1002/joc.3370100202, 1990.

Lehning, M., Bartelt, P., Brown, B., Fierz, C. and Satyawali, P. A physical SNOWPACK model for the Swiss avalanche warning: Part II. Snow microstructure. Cold regions science and technology, 35(3), 147-167, https://doi.org/10.1016/S0165-232X(02)00073-3, 2002.

Leppänen, L., Kontu, A., Hannula, H.-R., Sjöblom, H., and Pulliainen, J.: Sodankylä manual snow survey program, Geosci. Instrum. Method. Data Syst., 5, 163-179, https://doi.org/10.5194/gi-5-163-2016, 2016.

Lievens, H., Demuzere, M., Marshall, H.P., Reichle, R.H., Brucker, L., Brangers, I., de Rosnay, P., Dumont, M., Girotto, M., Immerzeel, W.W. and Jonas, T., 2019. Snow depth variability in the Northern Hemisphere mountains observed from space. Nature communications, 10(1), pp.1-12.

Liu, Y.; Li, L.; Yang, J.; Chen, X.; Hao, J. Estimating Snow Depth Using Multi-Source Data Fusion Based on the D-InSAR Method and 3DVAR Fusion Algorithm. Remote Sens., 9, 1195, https://doi.org/10.3390/rs9111195, 2017.

Lundberg, A., Granlund, N. and Gustafsson, D. Towards automated 'Ground truth'snow measurements—A review of operational and new measurement methods for Sweden, Norway, and Finland. Hydrological processes, 24(14), 1955-1970, https://doi.org/10.1002/hyp.7658, 2010.

Marty, C. and Meister, R. Long-term snow and weather observations at Weissfluhjoch and its relation to other high-altitude observatories in the Alps. Theoretical and Applied Climatology, 110(4), 573-583, https://doi.org/10.1007/s00704-012-0584-3, 2012.

Mastrotheodoros, T., Pappas, C., Molnar, P. et al. More green and less blue water in the Alps during warmer summers. Nat. Clim. Chang. 10, 155–161, https://doi.org/10.1038/s41558-019-0676-5, 2020.

Mizukami, N. and Perica, S. Spatiotemporal characteristics of snowpack density in the mountainous regions of the western United States. Journal of Hydrometeorology, 9(6), 1416-1426, https://doi.org/10.1175/2008JHM981.1, 2008.

Morin, S., Lejeune, Y., Lesaffre, B., Panel, J.-M., Poncet, D., David, P., and Sudul, M.: An 18-yr long (1993–2011) snow and meteorological dataset from a mid-altitude mountain site (Col de Porte, France, 1325 m alt.) for driving and evaluating snowpack models, Earth Syst. Sci. Data, 4, 13-21, https://doi.org/10.5194/essd-4-13-2012, 2012.

Papa, F., Legresy, B., Mognard, N.M., Josberger, E.G. and Remy, F. Estimating terrestrial snow depth with the TOPEX-Poseidon altimeter and radiometer. IEEE Transactions on Geoscience and Remote Sensing, 40(10), 2162-2169, doi: 10.1109/TGRS.2002.802463, 2002.

Parajka, J., Haas, P., Kirnbauer, R., Jansa, J. and Blöschl, G. Potential of time-lapse photography of snow for hydrological purposes at the small catchment scale. Hydrological Processes, 26(22), 3327-3337, https://doi.org/10.1002/hyp.8389, 2012.

Peltoniemi , M., Aurela , M., Bottcher , K., Kolari , P., Loehr , J., Karhu , J., Linkosalmi , M., Tanis , C.M., Tuovinen , J.P. & Arslan , A.N..Webcam network and image database for studies of phenological changes of vegetation and snow cover in Finland, image time series from 2014 to 2016. Earth system science data , vol. 10 , no. 1 , 173-184, https://doi.org/10.5194/essd-10-173-2018, 2018.

Pirazzini, R., Leppänen, L., Picard, G., Lopez-Moreno, J., Marty, C., Macelloni, G., Kontu, A., von Lerber, A., Tanis, C., Schneebeli, M. and de Rosnay, P. European in-situ snow measurements: Practices and purposes. Sensors, 18(7), 2016, https://doi.org/10.3390/s18072016, 2018.

Qiao, D., Li, Z., Nianqin, W., Zhou, J., Zhang, P. and Gao, S. Validation of the daily passive microwave snow depth products over northern china. International Archives of the Photogrammetry, Remote Sensing & Spatial Information Sciences, 42(3), https://doi.org/10.5194/isprs-archives-XLII-3-1401-2018, 2018.

Rasmussen, R.M., Hallett, J., Purcell, R., Landolt, S.D. and Cole, J. The hotplate precipitation gauge. Journal of Atmospheric and Oceanic Technology, 28(2), 148-164, https://doi.org/10.1175/2010JTECHA1375.1, 2011.

Sevruk, B.O.R.I.S. Point precipitation measurements why are they not corrected. Water for the Future: Hydrology in Perspective (Proceedings of the Rome Symposium, April 1987). IAHS Publ. no. 164, 447-457, 1987.

Tanis, C., Peltoniemi, M., Linkosalmi, M., Aurela, M., Böttcher, K., Manninen, T. and Arslan, A. A system for acquisition, processing and visualization of image time series from multiple camera networks. Data, 3(3), 23, https://doi.org/10.3390/data3030023, 2018.

Takala, M., Luojus, K., Pulliainen, J., Derksen, C., Lemmetyinen, J., Kärnä, J.P., Koskinen, J. and Bojkov, B.. Estimating northern hemisphere snow water equivalent for climate research through assimilation of space-borne radiometer data and ground-based measurements. Remote Sensing of Environment, 115(12), 3517-3529, https://doi.org/10.1016/j.rse.2011.08.014, 2011.

Tedesco, M. Remote sensing of the cryosphere. John Wiley & Sons, Cryosphere Science Series, 2014.

Vander Jagt, B., Lucieer, A., Wallace, L., Turner, D. and Durand, M. Snow depth retrieval with UAS using photogrammetric techniques. Geosciences, 5(3), 264-285, https://doi.org/10.3390/geosciences5030264, 2015.

Vionnet, V., Brun, E., Morin, S., Boone, A., Faroux, S., Le Moigne, P., Martin, E., and Willemet, J.-M.: The detailed snowpack scheme Crocus and its implementation in SURFEX v7.2, Geosci. Model Dev., 5, 773-791, https://doi.org/10.5194/gmd-5-773-2012, 2012.

Wever, N., Fierz, C., Mitterer, C., Hirashima, H., and Lehning, M.: Solving Richards Equation for snow improves snowpack meltwater runoff estimations in detailed multi-layer snowpack model, The Cryosphere, 8, 257-274, https://doi.org/10.5194/tc-8-257-2014, 2014.

Wever, N., Schmid, L., Heilig, A., Eisen, O., Fierz, C., and Lehning, M.: Verification of the multi-layer SNOWPACK model with different water transport schemes, The Cryosphere, 9, 2271-2293, https://doi.org/10.5194/tc-9-2271-2015, 2015.